

# Organometallic Titanocene–Gold Compounds as Potential Chemotherapeutics in Renal Cancer. Study of their Protein Kinase Inhibitory Properties

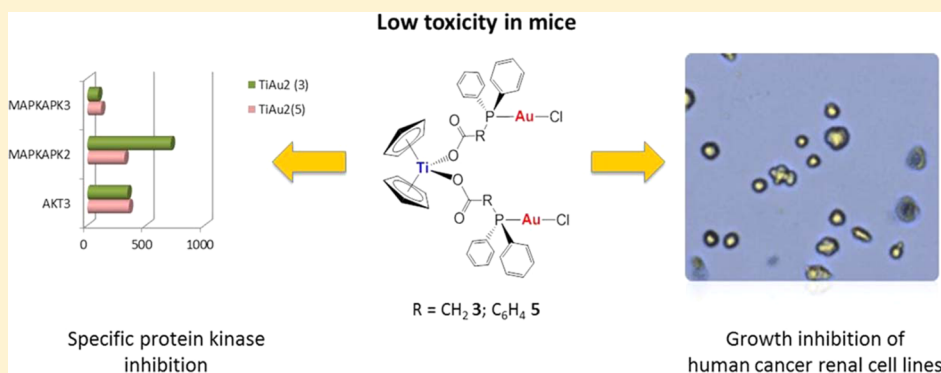
Jacob Fernández-Gallardo,<sup>†</sup> Benelita T. Elie,<sup>†</sup> Florian J. Sulzmaier,<sup>‡,⊥</sup> Mercedes Sanaú,<sup>§</sup> Joe W. Ramos,<sup>\*,‡</sup> and María Contel<sup>\*,†,‡</sup>

<sup>†</sup>Department of Chemistry, Brooklyn College and The Graduate Center, The City University of New York, Brooklyn, New York 11210, United States

<sup>‡</sup>Cancer Biology Program, University of Hawaii Cancer Center, University of Hawaii at Manoa, Honolulu, Hawaii 96813, United States

<sup>§</sup>Departamento de Química Inorgánica, Universidad de Valencia, Burjassot, Valencia, 46100, Spain

## S Supporting Information



**ABSTRACT:** Early–late transition metal TiAu<sub>2</sub> compounds [( $\eta$ -C<sub>5</sub>H<sub>5</sub>)<sub>2</sub>Ti{OC(O)CH<sub>2</sub>PPh<sub>2</sub>AuCl}]<sub>2</sub> (3) and new [( $\eta$ -C<sub>5</sub>H<sub>5</sub>)<sub>2</sub>Ti{OC(O)-4-C<sub>6</sub>H<sub>4</sub>PPh<sub>2</sub>AuCl}]<sub>2</sub> (5) were evaluated as potential anticancer agents *in vitro* against renal and prostate cancer cell lines. The compounds were significantly more effective than monometallic titanocene dichloride and gold(I) [{HOC(O)RPPH<sub>2</sub>}AuCl] (R = -CH<sub>2</sub>- 6, -4-C<sub>6</sub>H<sub>4</sub>- 7) derivatives in renal cancer cell lines, indicating a synergistic effect of the resulting heterometallic species. The activity on renal cancer cell lines (for 5 in the nanomolar range) was considerably higher than that of cisplatin and highly active titanocene Y. Initial mechanistic studies in Caki-1 cells *in vitro* coupled with studies of their inhibitory properties on a panel of 35 kinases of oncological interest indicate that these compounds inhibit protein kinases of the AKT and MAPKAPK families with a higher selectivity toward MAPKAPK3 (IC<sub>50</sub> 3 = 91 nM, IC<sub>50</sub> 5 = 117 nM). The selectivity of the compounds *in vitro* against renal cancer cell lines when compared to a nontumorigenic human embryonic kidney cell line (HEK-293T) and the favorable preliminary toxicity profile on C57black6 mice indicate that these compounds (especially 5) are excellent candidates for further development as potential renal cancer chemotherapeutics.

## INTRODUCTION

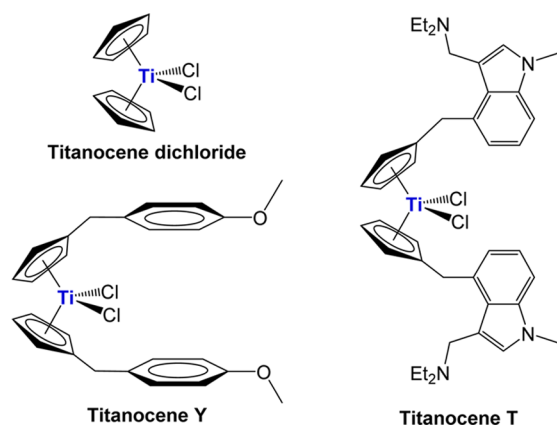
Cisplatin and the follow-on drugs carboplatin (paraplatin) and oxaliplatin (eloxatin) are used to treat 40–80% of cancer patients alone or in combination chemotherapy.<sup>1</sup> However, their effectiveness is still hindered by clinical problems, including acquired or intrinsic resistance, a limited spectrum of activity, and high toxicity leading to side effects.<sup>1,2</sup> Promising anticancer activities of a variety of other metal complexes have been reported in the past two decades.<sup>3–8</sup> Metallocene dihalides (Cp<sub>2</sub>MCl<sub>2</sub>, Cp = cyclopentadienyl, M = Ti, V, Nb, Mo, Re) were the first organometallic compounds with antitumor properties to be identified.<sup>9,10</sup> Titanocene dichloride (Cp<sub>2</sub>TiCl<sub>2</sub>, Chart 1) was the first organometallic complex to enter clinical trials in 1993.<sup>11</sup> Cp<sub>2</sub>TiCl<sub>2</sub> exhibited considerable

antitumor activity in *in vitro* and *in vivo* experimental models even against cisplatin-resistant cells and tumors generally difficult to treat.<sup>12,13</sup> However, the efficacy of Cp<sub>2</sub>TiCl<sub>2</sub> in phase II clinical trials in patients with metastatic renal cell carcinoma<sup>14</sup> or metastatic breast cancer was too low to be pursued.<sup>15</sup>

During the past years there has been a renewed interest in the potential of more stable titanocene complexes as anticancer agents.<sup>16</sup> The most promising candidates have been compounds described by the group of M. Tacke in Dublin.<sup>17–22</sup> Substituted titanocenes such as Titanocene Y (Chart 1) have

Received: September 21, 2014

Published: October 30, 2014

**Chart 1. Selected Organometallic Titanium Derivatives with Relevant Antitumor Properties**

shown activity *in vivo* against human breast<sup>18</sup> and epidermoid carcinoma<sup>19</sup> xenografts in mice.

The *in vivo* studies on human renal cancer cells (Caki-1) in mice with Titanocene Y,<sup>20</sup> Titanocene Y\*,<sup>21</sup> and recently described water-soluble Titanocene T<sup>22</sup> (Chart 1) have shown significant tumor inhibition, which may lead to clinical tests against metastatic renal cancer.

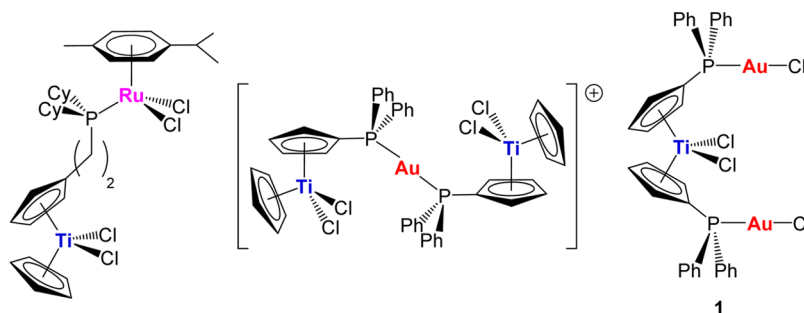
Another promising family of metallodrugs for cancer chemotherapy is that of gold complexes. In particular, a number of gold compounds have overcome cisplatin resistance to specific cancer cells,<sup>23,24</sup> which makes them attractive potential therapeutics. In addition, it has been found that DNA is not the primary target for most gold compounds,<sup>25</sup> reinforcing the idea that their mode of action is different than that of cisplatin. The inhibition of mitochondrial enzymes and of the proteasome for gold compounds has been reported.<sup>26,27</sup> Histone deacetylases, mTor, cathepsin cysteine proteases, and PKC and cyclin-dependent kinases have been proposed as possible biochemical targets for some of the gold(III) and gold(I) complexes.<sup>28–31</sup> Gold(I)–thiolate compounds (such as aurothiomalate) inhibit the protein kinase PKC $\epsilon$ ,<sup>32,33</sup> while auranofin is known to inhibit I $\kappa$ B kinase (IKK).<sup>34</sup> More recently, gold compounds have been found to efficiently inhibit PARP-1 (poly(ADP-ribose) polymerase-1).<sup>35–37</sup>

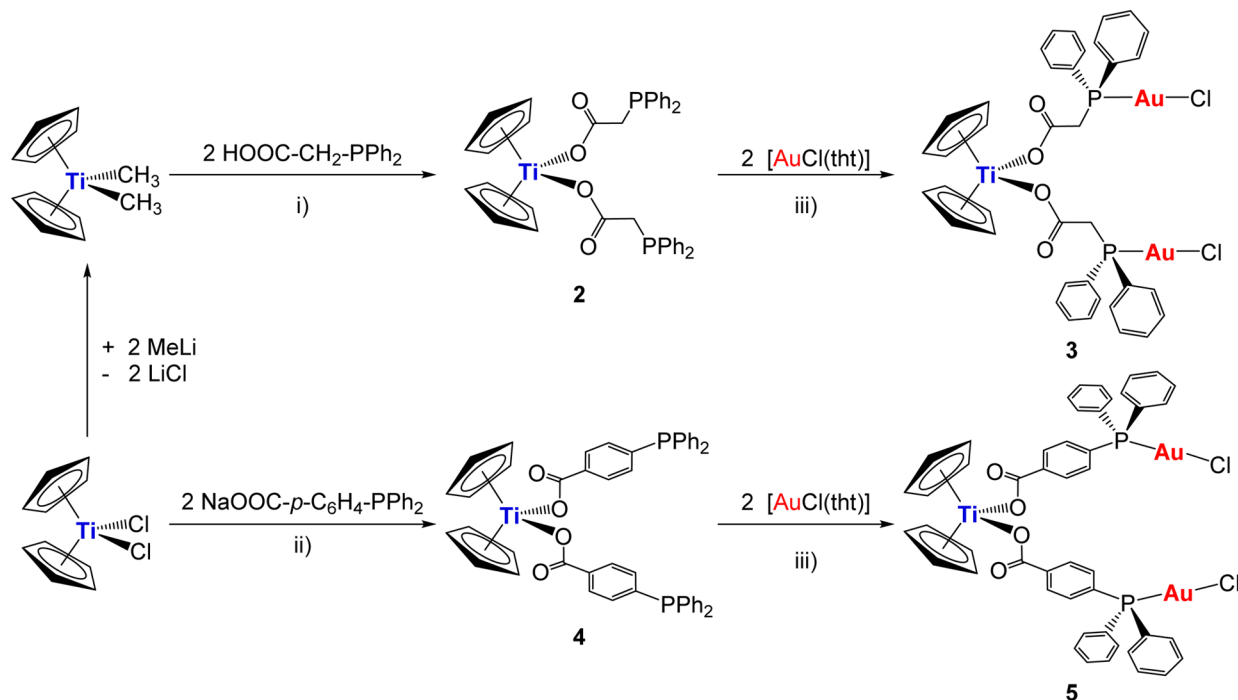
Within the frame of exploring compounds that may overcome cisplatin resistance, there has been a growing interest in heterometallic complexes as potential anticancer agents.<sup>37</sup> The hypothesis is that the incorporation of two different cytotoxic metals in the same molecule may improve their activity as antitumor agents due to interaction of the different

metals with multiple biological targets or by the improved chemophysical properties of the resulting heterometallic compound. Early–late transition metal complexes have been the subject of research due to their potential in catalysis.<sup>38</sup> We and others have reported on early–late transition metal compounds based on titanocene fragments (Ru–Ti<sup>39</sup> and Ti–Au<sup>40,41</sup> in Chart 2). These compounds showed a cytotoxic effect on human ovarian<sup>39–41</sup> and prostate<sup>41</sup> cancer cell lines and were more active than their Ti or M (Ru or Au) separate monometallic fragments.

It has been proposed that titanocene dichloride hydrolyzes at pH 7, liberating the Cp rings<sup>42</sup> and binding to transferrin to get transported into the tumor cells and released by a nonredox mode of action (different from that of iron).<sup>43</sup> Thus, the heterometallic compounds previously described<sup>39–41</sup> could potentially break into monometallic species in physiological media or *in vivo* before reaching the tumors. We hypothesized that incorporating the second metal to a ligand strongly bound to the titanium(IV) center would ensure that heterometallic Ti–M species remain after the Ti–Cp hydrolysis takes place under physiological pH conditions. Since Ti–O bonds are considerably stronger ( $\Delta H_{f298} = 662(16)$  kJ/mol) than Ti–C ( $\Delta H_{f298} = 439$  kJ/mol) or Ti–Cl ( $\Delta H_{f298} = 494$  kJ/mol) bonds, we envisioned a carboxylate as the ideal group to bind titanium(IV) centers. Indeed, a compound in which gold–diphenylphosphinoacetate fragments had been coordinated to a titanocene moiety to generate a TiAu<sub>2</sub> heterometallic species<sup>44</sup> was described in 2000 (3 in Scheme 1).

We report here on the synthesis and characterization of a related compound with a more rigid structure (5 in Scheme 1) as well as the complete characterization of 3 (including its crystal structure). The stability of these compounds over time in DMSO-*d*<sub>6</sub> (dimethyl sulfoxide) and PBS (phosphate buffer saline) solution has been monitored by NMR and UV–vis spectroscopy, respectively. We describe preliminary biological data on their *in vitro* activity against human renal (A498, UO31, Caki-1) and prostate (PC3, DU145) cancer cell lines and a nontumorigenic human embryonic kidney cell line (HEK-293T). The compounds induced cell death, and the type of cell death (apoptosis versus necrosis) has been investigated. The compounds were also tested for their possible interactions with plasmid (pBR322) DNA used as a model nucleic acid. More importantly, we present a study of the inhibitory effects of some titanocene–gold TiAu<sub>2</sub> compounds (1, 3) and titanocene dichloride against a panel of 34 protein kinases of oncological interest and verify activity in cancer cell lines against these targets. In addition, we include preliminary toxicity data of compounds 3 and 5 on C57black6 mice.

**Chart 2. Selected Heterometallic Titanocene–Ruthenium and Titanocene–Gold Derivatives with Antiproliferative Activities against Human Ovarian<sup>39,40</sup> and Prostate<sup>41</sup> Cancer Cell Lines**

Scheme 1. Preparation of Heterometallic Titanocene–Gold Complexes  $[(\eta\text{-C}_5\text{H}_5)_2\text{Ti}\{\text{OC}(\text{O})\text{RPPh}_2\text{AuCl}\}_2]^a$ 

<sup>a</sup>R =  $-\text{CH}_2-$  3;<sup>44</sup>  $-4\text{-C}_6\text{H}_4-$  5; (i)  $\text{CH}_2\text{Cl}_2$  RT, 6 h; (ii)  $\text{CHCl}_3$  RT, 1.5 h; (iii)  $\text{CH}_2\text{Cl}_2$  RT.

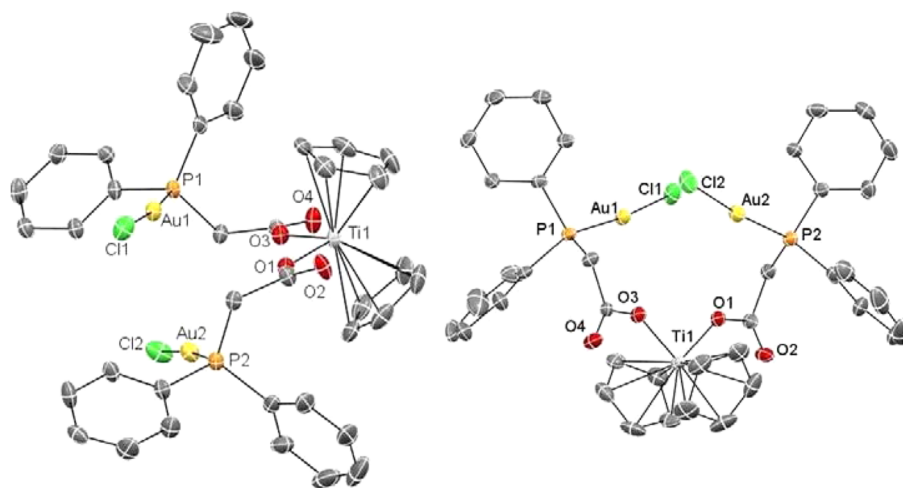


**Figure 1.** Two ORTEP views of the molecular structure of **3** showing the labeling scheme. Labeling for hydrogen and carbon atoms is omitted for clarity. A drawing of the molecular structure containing carbon atoms labeled is provided in the SI.

## RESULTS AND DISCUSSION

**1. Synthesis and Characterization.** The synthesis of heterometallic compound  $\text{TiAu}_2$  **3** has been performed following the procedure previously described.<sup>44</sup> The reaction of  $[\text{Cp}_2\text{TiMe}_2]$  and 2 equiv of acid  $[\text{PPh}_2\text{-CH}_2\text{-CO}_2\text{H}]$  generates the titanocene species with phosphino acetate ligands  $[(\eta\text{-C}_5\text{H}_5)_2\text{Ti}\{\text{OC}(\text{O})\text{CH}_2\text{PPh}_2\}_2]$  (R =  $-\text{CH}_2-$  **2**<sup>44</sup>) with concomitant elimination of methane (Scheme 1).

Remarkably, we were able to prepare new titanocene complex  $[(\eta\text{-C}_5\text{H}_5)_2\text{Ti}\{\text{OC}(\text{O})\text{-4-C}_6\text{H}_4\text{PPh}_2\}_2]$ , **4**, starting from commercially available  $[\text{Cp}_2\text{TiCl}_2]$  and the sodium salt  $[\text{PPh}_2\text{-4-C}_6\text{H}_4\text{-CO}_2\text{Na}]$ , which eliminates the need for using  $[\text{Cp}_2\text{TiMe}_2]$ . The reaction to obtain **2** starting from  $[\text{Cp}_2\text{TiCl}_2]$  and the corresponding sodium salt  $[\text{PPh}_2\text{-CH}_2\text{-CO}_2\text{Na}]$  was unsuccessful. Both **2** and **4** are obtained as yellow solids in high

yields. Addition of 2 equiv of  $[\text{AuCl}(\text{tht})]$  to titanocenes **2**<sup>44</sup> and **4** affords the heterometallic complexes  $[(\eta\text{-C}_5\text{H}_5)_2\text{Ti}\{\text{OC}(\text{O})\text{RPPh}_2\text{AuCl}\}_2]$  (R =  $-\text{CH}_2-$  **3**,<sup>44</sup>  $-4\text{-C}_6\text{H}_4-$  **5**) in moderate to high yields. Compounds **3** and **5** are obtained as pale yellow, air- and moisture-stable solids, which can be kept at low temperatures (fridge) for months. Titanocenes **2** and **4** and the heterometallic compounds **3** and **5** are less acidic than titanocene dichloride (Experimental Section). The compounds are soluble in DMSO/ $\text{H}_2\text{O}$  (1:99) mixtures at micromolar concentrations, which is relevant for subsequent biological testing. The structures in Scheme 1 have been proposed based on published<sup>44</sup> spectroscopic and analytical results for compounds **2** and **3**, crystallographic data for **2**,<sup>44</sup> and on our own results for **4** and **5** (see Experimental Section).

**Table 1.** Selected Structural Parameters of Complex **3** Obtained from X-ray Single-Crystal Diffraction Studies (Bond Lengths in Å and Angles in deg)

Ti(1)–O(1)	1.962(10)	Ti(1)–O(3)	1.957(10)
O(1)–C(2)	1.302(17)	O(3)–C(4)	1.310(17)
O(2)–C(2)	1.169(17)	O(4)–C(4)	1.188(17)
C(2)–C(1)	1.56(2)	C(4)–C(3)	1.51(2)
Au(2)–P(2)	2.226(4)	Au(1)–P(1)	2.222(4)
Au(2)–Cl(2)	2.279(4)	Au(1)–Cl(1)	2.287(4)
Ti(1)–O(1)	1.962(10)	Ti(1)–O(3)	1.957(10)
O(1)–C(2)	1.302(17)	O(3)–C(4)	1.310(17)
O(2)–C(2)	1.169(17)	O(4)–C(4)	1.188(17)
C(2)–C(1)	1.56(2)	C(4)–C(3)	1.51(2)
Au(2)–P(2)	2.226(4)	Au(1)–P(1)	2.222(4)
Au(2)–Cl(2)	2.279(4)	Au(1)–Cl(1)	2.287(4)
average Ti(1)–C(21–25)	2.381(2)	average C–C in Cp ring C(21)–C(25)	1.386(3)
average Ti(1)–C(11–15)	2.385(2)	average C–C in Cp ring C(11)–C(15)	1.392(3)
distance Ti–Z (centroid of Cp)	2.069		
Ti(1)–O(3)–C(4)	141.0(9)	C23–Ti1–C12	171.9(7)
O(1)–Ti(1)–O(3)	95.8(4)	O(3)–C(4)–O(4)	123.0(13)
Ti(1)–O(1)–C(2)	137.2(9)	O(4)–C(4)–C(3)	122.6(14)
C15–Ti1–C21	100.9(9)	C(3)–C(4)–P(1)	111.5(11)
O(1)–C(2)–O(2)	126.5(15)	P(2)–Au(2)–Cl(2)	173.71(19)
O(2)–C(2)–C(1)	122.1(14)	P(1)–Au(1)–Cl(1)	173.15(17)
C(1)–C(2)–P(2)	112.8(11)		

The crystal structure of **3** has been determined by an X-ray diffraction study confirming that there are two molecules of gold(I)–chloride–phosphino acetate coordinated to the titanocene moiety through one of the oxygen atoms of the carboxylate ligand. Figure 1 depicts two different views of the molecule in compound **3**, and selected bond distances and angles are collected in Table 1 (crystallographic details can be found in the SI).

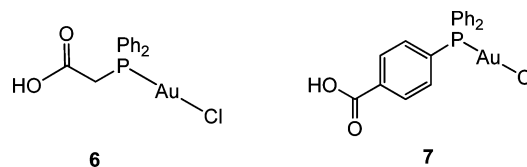
The structure of titanocene attached to the two phosphine–acetate ligands is very similar to that of  $[(\eta\text{-C}_5\text{H}_5)_2\text{Ti}\{\text{OC}(\text{O})\text{-CH}_2\text{PPh}_2\}_2\text{PdCl}_2]$ .<sup>44</sup> As in the Pd structure, the monodentate carboxylate coordination is also indicated by the significant differences in C–O bond lengths depending on whether the oxygen is coordinated to titanium [1.962(10); 1.957(10) Å] or not [3.460(11), 3.486(11) Å]. The titanium has a distorted tetrahedral environment comprising two cyclopentadienyl rings, the Z–Ti–Z angle being 132.89° and the O(1)–Ti–O(3) angle 95.8(4)°. The gold atoms are in a quasi linear arrangement (P(1)–Au(1)–Cl(1) 173.15(17)° and P(2)–Au(2)–Cl(2) 173.71(19)°). The distances Au–P and Au–Cl (Table 1) are almost identical to the distances found in complex  $[\{\text{HOC}(\text{O})\text{CH}_2\text{PPh}_2\}\text{AuCl}]$  (**6**),<sup>45</sup> of 2.220(2) and 2.270(3) Å, respectively, and are in the range of many other gold–phosphino chloride derivatives described in the literature. There is no contact Au–Au, as the distance found is 3.693 Å.

The stability of the compounds has been evaluated by  $^{31}\text{P}\{^1\text{H}\}$  and  $^1\text{H}$  NMR spectroscopy in DMSO- $d_6$  and by vis–UV spectroscopy in DMSO/PBS solution over time (see SI). As reported for titanocene dichloride, compounds **3** and **5** lose the cyclopentadienyl groups in DMSO (most plausibly being replaced by OH groups).<sup>42</sup> We studied a solution of **3** in 50:50 DMSO- $d_6$ /D $_2$ O by  $^{31}\text{P}\{^1\text{H}\}$  and  $^1\text{H}$  NMR spectroscopy, and we observed that **3** is stable for 24 h with a half-life of 48 h, indicating that the compound is more stable in D $_2$ O than in DMSO (see Figures S16 and S17 in the SI). Titanocene dichloride is also known to hydrolyze much faster in DMSO than in water.<sup>42</sup> Compound **5** precipitated in a 50:50 DMSO-

$d_6$ /D $_2$ O solution in the amount necessary to perform NMR spectroscopy. The vis–UV of compounds **3** and **5** (micromolar concentration) in 1:99 DMSO/PBS solution do not change much over time (24 h, Figures S21 and S.23 in the SI). Mass spectrometry also indicates the presence of species containing both titanium and gold in 1% DMSO/PBS solution after 24 h (Figures S24–S33 in the SI). We used micromolar solutions of **3** and **5** in DMSO/media or DMSO/PBS (1:99) for subsequent biological testing.

## 2. Biological Activity. 2.1. Cytotoxicity and Cell Death.

The cytotoxicity of the heterometallic complexes  $[(\eta\text{-C}_5\text{H}_5)_2\text{Ti}\{\text{OC}(\text{O})\text{RPPH}_2\text{AuCl}\}_2]$  (R =  $-\text{CH}_2-$  **3**;<sup>44</sup>  $-4\text{-C}_6\text{H}_4-$  **5**) and monometallic gold(I) complexes  $[\text{HOC}(\text{O})\text{RPPH}_2\text{AuCl}]$  (R =  $-\text{CH}_2-$  **6**;<sup>45</sup>  $-4\text{-C}_6\text{H}_4-$  **7** in Figure 2) was assayed by monitoring their ability to inhibit cell growth using the XTT assay (see the Experimental Section).

**Figure 2.** Structures of monometallic  $[\{\text{HOC}(\text{O})\text{RPPH}_2\}\text{AuCl}]$  (R =  $-\text{CH}_2-$  **6**;<sup>45</sup>  $-4\text{-C}_6\text{H}_4-$  **7**).

The cytotoxic activity of the compounds was determined as described in the Experimental Section in the human renal cancer A498, UO31, and Caki-1 cell lines and in the human prostate cancer PC3 and DU-145 cell lines, in comparison to cisplatin, titanocene dichloride (Chart 1), and Titanocene Y<sup>46</sup> (Chart 1). The results are summarized in Table 2.

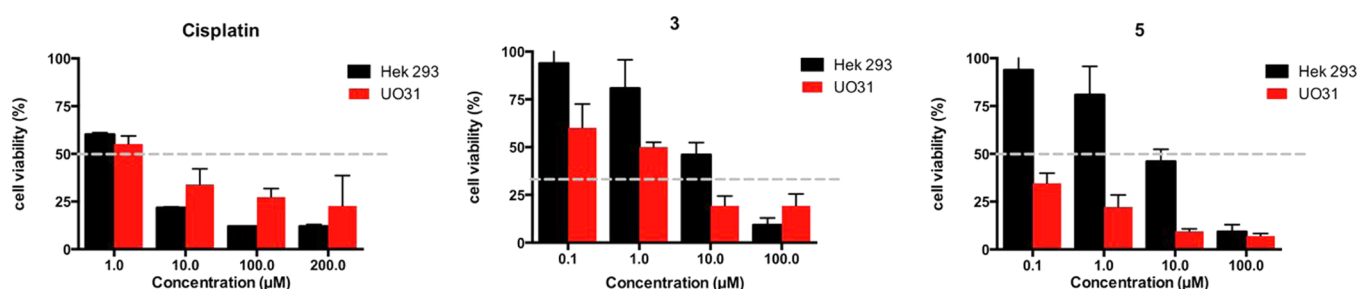
We had previously reported<sup>41</sup> on the cytotoxic activity of  $[\text{TiCl}_2\{\eta^5\text{-C}_5\text{H}_4\text{PPh}_2(\text{AuCl})\}_2]$  (**1**) in human ovarian (IC<sub>50</sub> 24 h = 2.44 μM) and prostate cancer cell line DU145 (IC<sub>50</sub> 24 h = 27.26 μM), and we did a preliminary evaluation of **1** in human prostate cancer cell line PC3, human renal cancer cell line



**Table 2.** IC<sub>50</sub> (μM) of Heterometallic TiAu<sub>2</sub> Compounds **3** and **5**, Monometallic Au **6** and **7**, Cisplatin, Titanocene Dichloride, and Titanocene Y in Human Cell Lines<sup>a</sup>

	A498	UO31	Caki-1	HEK-293T	PC3	DU145
[Cp <sub>2</sub> Ti{OC(O)CH <sub>2</sub> PPh <sub>2</sub> AuCl} <sub>2</sub> ], <b>3</b>	8.7 ± 1.7 (24 h) 3.2 ± 0.38 (72 h)	6.3 ± 1.1 (24 h) 1.4 ± 0.1 (72 h)	6.0 ± 1.8 (24 h) 2.2 ± 0.99 (72 h)	24 ± 0.73 (24 h) 6.9 ± 2.4 (72 h)	51.7 ± 4.2 (24 h) 27.1 ± 4 (72 h)	38.6 ± 5.5 (24 h) 35.5 ± 1.4 (72 h)
[HOC(O)CH <sub>2</sub> PPh <sub>2</sub> AuCl], <b>6</b>	58 ± 11.0 (24 h) 43 ± 4.9 (72 h)	27.3 ± 2.7 (24 h) 5.2 ± 1.6 (72 h)	33.8 ± 2.1 (24 h) 23.0 ± 4.1 (72 h)	36.5 ± 3.3 (24 h) 9.7 ± 2.5 (72 h)	38.2 ± 2.2 (24 h) 30.2 ± 4.2 (72 h)	34.7 ± 1.8 (24 h) 31.3 ± 3.1 (72 h)
[Cp <sub>2</sub> Ti{OC(O)-4-C <sub>6</sub> H <sub>4</sub> PPh <sub>2</sub> AuCl} <sub>2</sub> ], <b>5</b>	28 ± 3.4 (24 h) 6.9 ± 2.2 (72 h)	6.8 ± 0.2 (24 h) 0.3 ± 0.06 (72 h)	10.3 ± 4.1 (24 h) 1.0 ± 0.29 (72 h)	39 ± 4.1 (24 h) 20.1 ± 1.6 (72 h)	51 ± 4.2 (24 h) 37.7 ± 7.1 (72 h)	33.4 ± 1.8 (24 h) 6.6 ± 1.8 (72 h)
[HOC(O)-4-C <sub>6</sub> H <sub>4</sub> PPh <sub>2</sub> AuCl], <b>7</b>	36.1 ± 6.3 (24 h) 21 ± 2.5 (72 h)	38.3 ± 4.1 (24 h) 1.2 ± 0.8 (72 h)	28.4 ± 5.9 (24 h) 19.2 ± 2.9 (72 h)	34.2 ± 3.7 (24 h) 31 ± 0.9 (72 h)	>200 (24 h) 78 ± 18.1 (72 h)	32 ± 2.7 (24 h) 39 ± 5.7 (72 h)
cisplatin	74.7 ± 6.0 (24 h) 37.2 ± 4.6 (72 h)	>100 (24 h) 8.9 ± 2.7 (72 h)	68.8 ± 0.14 (24 h) 29 ± 4.1 (72 h)	64.4 ± 7.9 (24 h) 3.2 ± 0.13 (72 h)	92 ± 18 (24 h) 14 ± 2.3 (72 h)	44.5 ± 0.33 (24 h) 12.1 ± 3.9 (72 h)
[Cp <sub>2</sub> TiCl <sub>2</sub> ] titanocene dichloride	>200 (24 h) >200 (72 h)	>200 (24 h) >200 (72 h)	>200 (24 h) >200 (72 h)	>200 (24 h) >200 (72 h)	>200 (24 h) >200 (72 h)	>200 (24 h) >200 (72 h)
Titanocene Y	>200 (24 h) >29.6 ± 2.8 (72 h)	>200 (24 h) >200 (72 h)	>200 (24 h) 29.4 ± 4.2 (72 h)	>200 (24 h) >200 (72 h)	>200 (24 h) 58.1 ± 11.2 (72 h)	>200 (24 h) 55.2 ± 7.9 (72 h)

<sup>a</sup>All compounds were dissolved in 1% of DMSO and diluted with water before addition to cell culture medium for a 24 or 72 h incubation period. Cisplatin and titanocene dichloride were dissolved in H<sub>2</sub>O. Data are expressed as mean ± SD (*n* = 3).

**Figure 3.** Selectivity of TiAu<sub>2</sub> compounds **3** and **5** between normal cells and cancer cells *in vitro*. The effects on cell viability of **3**, **5**, or cisplatin on UO31 and HEK-293T. UO31 and HEK-293T cells were seeded into a 96-well plate, and different concentrations of **3**, **5**, or cisplatin were then added to the cells after 24 h. The cell viability was measured by the XTT assay after the cells were treated with the compounds for 72 h.

A498, and nontumorigenic human MCF10A breast cancer cell line (IC<sub>50</sub> PC3 = 18.95 μM; IC<sub>50</sub> A498 = 16.26 μM; IC<sub>50</sub> MCF10A = 9.64 μM; XTT assay 20 h). However, the fact that **1** decomposes over time to species [AuClPPh<sub>2</sub>Cp], which are known to be cytotoxic but also poorly selective (as we observed when testing **1** on MCF10A), led us to focus attention on the study of heterometallic species **3** and **5** (Table 2). The heterometallic compounds **3** and **5** are more cytotoxic on renal cancer cell lines than on prostate cancer cell lines. In the case of prostate cancer cell lines the compounds are more toxic than cisplatin after 24 h, but only compound **5** is more toxic on DU145 after 72 h. They are also more toxic than titanocene dichloride and more toxic than Titanocene Y in these cell lines.

The heterometallic compounds are considerably more toxic to the renal cancer cell lines at both 24 and 72 h than cisplatin, titanocene dichloride, and even Titanocene Y. In addition, heterometallic compounds **3** and **5** are more toxic than the monometallic gold compounds on A498, UO31, and Caki-1 (both at 24 and 72 h), while being considerably less toxic to the nontumorigenic human embryonic kidney cell line (HEK-293T). This selectivity (see Figure 3) is especially pronounced for compound **5** on UO31 cells with an IC<sub>50</sub> value in the nanomolar range.

We studied the effect of the combination of monometallic compound **6** and titanocene dichloride in renal cancer cell lines at 24 h, which in all cases gave IC<sub>50</sub> values > 100 μM (data not shown). This fact supports the idea that there is indeed a

synergistic effect of the heterometallic complexes in their *in vitro* activity on renal cancer cell lines.

The trend for the monometallic complexes is not that clear. **6** is more toxic to prostate cell lines than to A498. **7** is more toxic to UO31 than to PC3 and DU145 cell lines and in general is poorly cytotoxic to prostate cell lines. Both **6** and **7** are more toxic to UO31 and Caki-1 with respect to the other cell lines studied.

In order to gain some insight into the type of cell death that the heterometallic complexes induce in the cancer cell lines, we performed cell death assays on Caki-1 cells with complexes **3** and **5** dissolved in 1% DMSO (see Experimental Section for details) and using 1% DMSO alone in media and staurosporine as controls. As cells may die through programmed cell death (apoptosis) or necrosis, the mode of death mediated by our compounds was investigated.

In early stages of apoptosis, one of the significant biochemical features is loss of plasma membrane phospholipid asymmetry, due to translocation of phosphatidylserine (PS) from the cytoplasmic to extracellular side. This characteristic allows detection of externalized PS by the specific binding of annexin V (FITC-conjugated). Apoptotic cell death will eventually result in the permeabilization of the cell membrane, allowing propidium iodide (PI) to stain DNA within the nucleus. Alternatively, necrotic cells are immediately permeable and stain positive for PI and PS with no intervening PS positive only step. As shown in Figure 3, each histogram is divided into four quadrants with the left top quadrant detecting necrotic

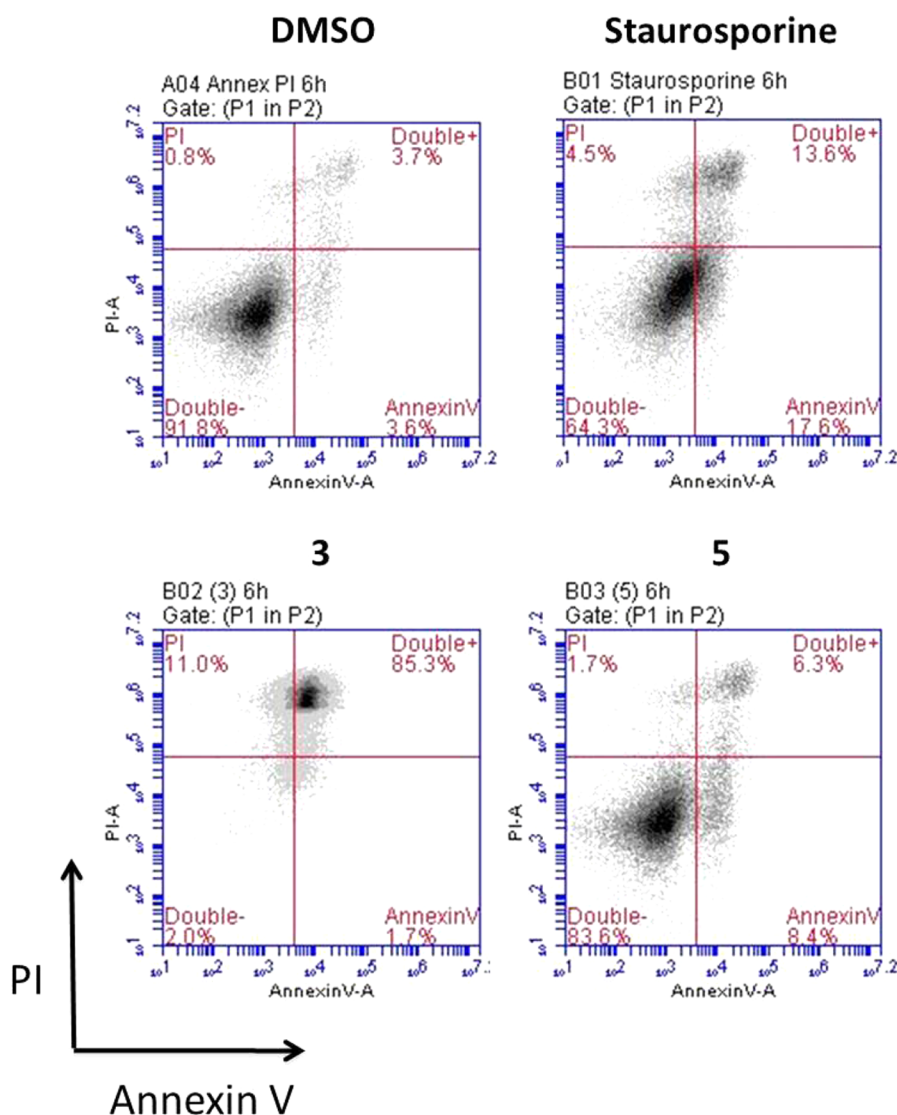


**Figure 4.** Cell death assays on Caki-1 cells induced by 3 and 5 ( $10 \mu\text{M}$ ) measured by using two-color flow cytometric analysis, after 6 h of incubation. 1% DMSO is vehicle alone control, and staurosporine is a known inducer of apoptosis as positive control.

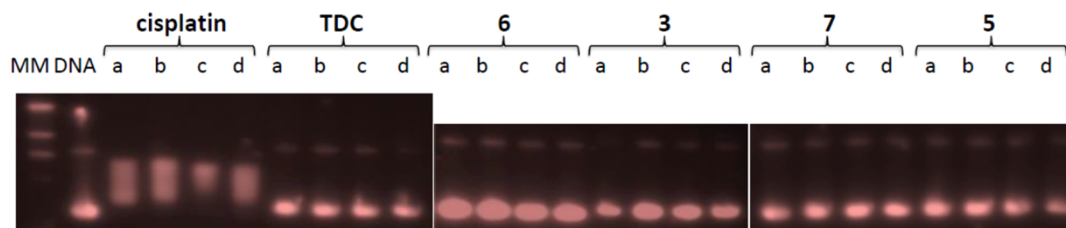


**Figure 5.** Electrophoresis mobility shift assays for cisplatin, titanocene dichloride, heterometallic  $\text{TiAu}_2$  compounds 3 and 5, and monometallic 6 and 7 (see Experimental Section for details). DNA refers to untreated plasmid pBR322. Letters a, b, c, and d correspond to metal/DNA ratios of 0.25, 0.5, 1.0, and 2.0, respectively.

cells without an annexin V-FITC signal. The right top quadrant shows cells with compromised membranes that are permeable to PI and stained with annexin V-FITC, which is indicative of necrosis and late apoptosis. The left bottom quadrant shows live cells that have intact membranes (not stained), while the right bottom quadrant represents cells that were stained (bound) with annexin V-FITC, which is indicative of early apoptosis. After incubation during 6 h with  $10 \mu\text{M}$  of compounds 3 and 5, necrosis can be clearly proposed for 3

(Figure 4). Compound 5 (with slower action on cancer cells, see *in vitro*  $\text{IC}_{50}$  values at 24 and 72 h) shows a pattern in accordance with apoptosis (compared to staurosporine, an apoptotic agent). Experiments at shorter (3) and longer (3 and 5) times are collected in the SI (Figures S34–S36), affording the same results. We are currently investigating the precise mechanism of cell death of these compounds. The induction of both apoptosis and necrosis are known for gold com-

pounds,<sup>47,48</sup> while titanocenes such as Titanocenes C, X, and Y are known to induce apoptosis in different cancer cell lines.<sup>13</sup>

**Interactions with Plasmid DNA.** Since DNA replication is a key event for cell division, it is among critically important targets in cancer chemotherapy. Most cytotoxic platinum drugs form strong covalent bonds with the DNA bases.<sup>49</sup> However, a variety of platinum compounds act as DNA intercalators upon coordination to the appropriate ancillary ligands.<sup>50</sup> DNA was believed to be the target for titanocene dichloride.<sup>42a</sup> Titanium accumulates in the cells in nuclear heterochromatin and, to a minor extent, in the nucleolus and ribosomes.<sup>51</sup> Titanium–DNA adducts were detected in A2780 cells treated with  $\text{Cp}_2\text{TiCl}_2$ , and this compound also inhibited DNA and RNA synthesis.<sup>52</sup> However, most recent reports on titanocene dichloride indicate that at physiological pH it neither binds strongly to DNA nor suppresses DNA-processing enzymes.<sup>53</sup> Titanocene Y has been recently shown to interact weakly with DNA.<sup>54</sup> As commented before, most gold-based compounds do not display a strong interaction with DNA.<sup>25</sup>

Thus, we performed agarose gel electrophoresis studies to unravel the effects of the heterometallic compounds **3** and **5**, monometallic gold(I) derivatives **6** and **7**, titanocene dichloride, and cisplatin on plasmid (pBR322) DNA (Figure 5). This plasmid has two main forms: OC (open circular or relaxed form, form II) and CCC (covalently closed or supercoiled form, form I). Changes in electrophoretic mobility of both forms are usually taken as evidence of metal–DNA binding. Generally, the larger the retardation of supercoiled DNA (CCC, form I), the greater the DNA unwinding produced by the drug.<sup>55</sup> Binding of cisplatin to plasmid DNA, for instance, results in a decrease in mobility of the CCC form and an increase in mobility of the OC form (see lanes a–d for cisplatin in Figure 5). Treatment with increasing amounts of monometallic Au(I) compounds **6** and **7** or heterometallic  $\text{TiAu}_2$  derivatives **3** and **5** does not affect the mobility of the faster-running supercoiled form (form I) even at the highest molar ratios (d). This is also in accordance with previously reported results on a titanocene–gold(I) phosphine derivative,  $[(\eta^5\text{-C}_5\text{H}_5)(\mu\text{-}\eta^5\text{-}k^1\text{-C}_5\text{H}_4\text{PPh}_2)_2\text{TiCl}_2]_2\text{Au}]\text{PF}_6$  (Chart 2), which did not interact with plasmid DNA.<sup>40</sup> We had found previously that titanocene dichloride does not interact with CT-DNA at physiological pH by CD spectroscopic studies.<sup>41</sup> Compounds of the type  $[\text{TiCl}_2\{\eta^5\text{-C}_5\text{H}_4\text{PPh}_2(\text{AuCl})\}_2]$  (**1**) displayed a stronger interaction with CT-DNA at pH 7 than titanocene dichloride.<sup>41</sup> However, the interaction was shown to be electrostatic in nature in accordance with the data for most gold compounds that show no or a weak interaction with DNA.<sup>25</sup>

The study of the interaction of these compounds at a more acidic or basic pH shows that there is no significant change with respect to neutral pH, and all the compounds do not interact with plasmid (pBR322) DNA (Figure 6).

**2.2. Protein Kinase Inhibition Studies and Initial Mechanistic Insights.** Protein kinases have an important role in oncogenesis and tumor progression, and they have therefore received increasing attention as targets for anticancer drugs, including recent and relevant examples of organometallic complexes (Meggers and co-workers).<sup>55–57</sup> In order to gain some mechanistic understanding of the mode of action of titanocene–gold derivatives, we tested the previously described compounds  $[\text{TiCl}_2\{\eta^5\text{-C}_5\text{H}_4\text{PPh}_2(\text{AuCl})\}_2]$ , **1**,  $[(\eta\text{-C}_5\text{H}_5)_2\text{Ti}\{\text{OC}(\text{O})\text{CH}_2\text{PPh}_2\text{AuCl}\}_2]$ , **3**, and titanocene dichloride  $[\text{Cp}_2\text{TiCl}_2]$  against a panel of 34 kinases of oncological interest

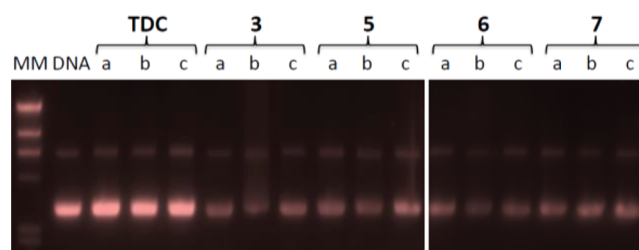


**Figure 6.** Electrophoresis mobility shift assays for titanocene dichloride and compounds **3**, **5**, **6**, and **7** at a metal/DNAbp ratio of 2.0 (see Experimental Section for details). DNA refers to untreated plasmid pBR322. Lanes a, b, and c correspond to pH 6, 7, and 8, respectively.

from the serine/threonine family (see Experimental Section for details). The graph in Figure 7 shows the inhibitory activity on 30 nonlipid kinases for titanocene chloride and compounds **1** and **3** at concentrations of 10  $\mu\text{M}$  (see Experimental Section for details).

The graph in Figure 8 shows the  $\text{IC}_{50}$  values (values at which 50% of the enzymatic activity is inhibited) on the four lipid PI3 kinases for titanocene dichloride. Compound **3** was inactive against the PI3 kinases even at values of 100  $\mu\text{M}$ , while the  $\text{IC}_{50}$  values for compound **1** ranged from 39.8 to 114.5  $\mu\text{M}$  and thus are not plotted in Figure 8. From this preliminary screening we narrowed down the panel of 30 kinases to those for which the compounds show an inhibitory effect of at least 50%. Titanocene dichloride did not inhibit the enzymatic activity to levels of 50% or below for any of these 30 kinases even at concentrations of 100  $\mu\text{M}$ . The  $\text{IC}_{50}$  values of **1** and **3** were subsequently calculated for the kinases in which they had an inhibitory effect of at least 50% (AKT1, AKT2, and AKT3 for **1** and **3**; ERK5/MAPK7 for **1**; and MAPKAPK2, MAPKAPK3, MAPKAPK5/PRAK, and PKCtheta for **3**).

Compound **1** inhibited ERK5/MAPK7 in the micromolar range ( $\text{IC}_{50} = 3.95 \mu\text{M}$ ), and the  $\text{IC}_{50}$  for compound **3** on PKCtheta was 11.6  $\mu\text{M}$ . Figure 9 shows the  $\text{IC}_{50}$  values below 1500 nM for **1** and/or **3** in specific kinases. From these studies we found that compounds **1** and **3** inhibit AKT protein kinases in the micromolar and nanomolar range (342 to 1425 nM). The AKT3 protein kinase is more effectively inhibited than AKT1 or AKT2 for both compounds (3.5 and 2.5 times, respectively).

In conclusion the inhibitory effects of titanocene dichloride and the heterometallic  $\text{TiAu}_2$  compounds **1** and **3** on protein kinases involved in cancer are very different. While titanocene dichloride inhibits exclusively protein kinases of the PI3 kinase family at nanomolar concentrations, compounds **1** (based on gold(I) fragments attached directly to the Cp rings of the titanocene,  $[\text{TiCl}_2\{\eta^5\text{-C}_5\text{H}_4\text{PPh}_2(\text{AuCl})\}_2]$ ) and **3** (based on titanocene attached to the gold(I) fragments through acetate groups  $[(\eta\text{-C}_5\text{H}_5)_2\text{Ti}\{\text{OC}(\text{O})\text{CH}_2\text{PPh}_2\text{AuCl}\}_2]$ ) inhibit in a similar manner protein kinases from the family AKT (especially AKT3). In addition, compound **3** inhibits protein kinases of the MAPKAPK families with  $\text{IC}_{50}$  in the nanomolar range for MAPKAPK2 (712 nM) and MAPKAPK3 (91 nM).

Compound **5**  $[(\eta\text{-C}_5\text{H}_5)_2\text{Ti}\{\text{OC}(\text{O})\text{-}4\text{-C}_6\text{H}_4\text{PPh}_2\text{AuCl}\}_2]$ , closely related to **3**, was tested against the three kinases for which **3** was most active, confirming that this type of  $\text{TiAu}_2$  compound inhibits AKT3 ( $\text{IC}_{50} = 355 \text{ nM}$ ), MAPKAPK2 ( $\text{IC}_{50} = 317 \text{ nM}$ ), and MAPKAPK3 ( $\text{IC}_{50} = 117 \text{ nM}$ ) very efficiently. In a separate experiment, we confirmed that compounds **3** and

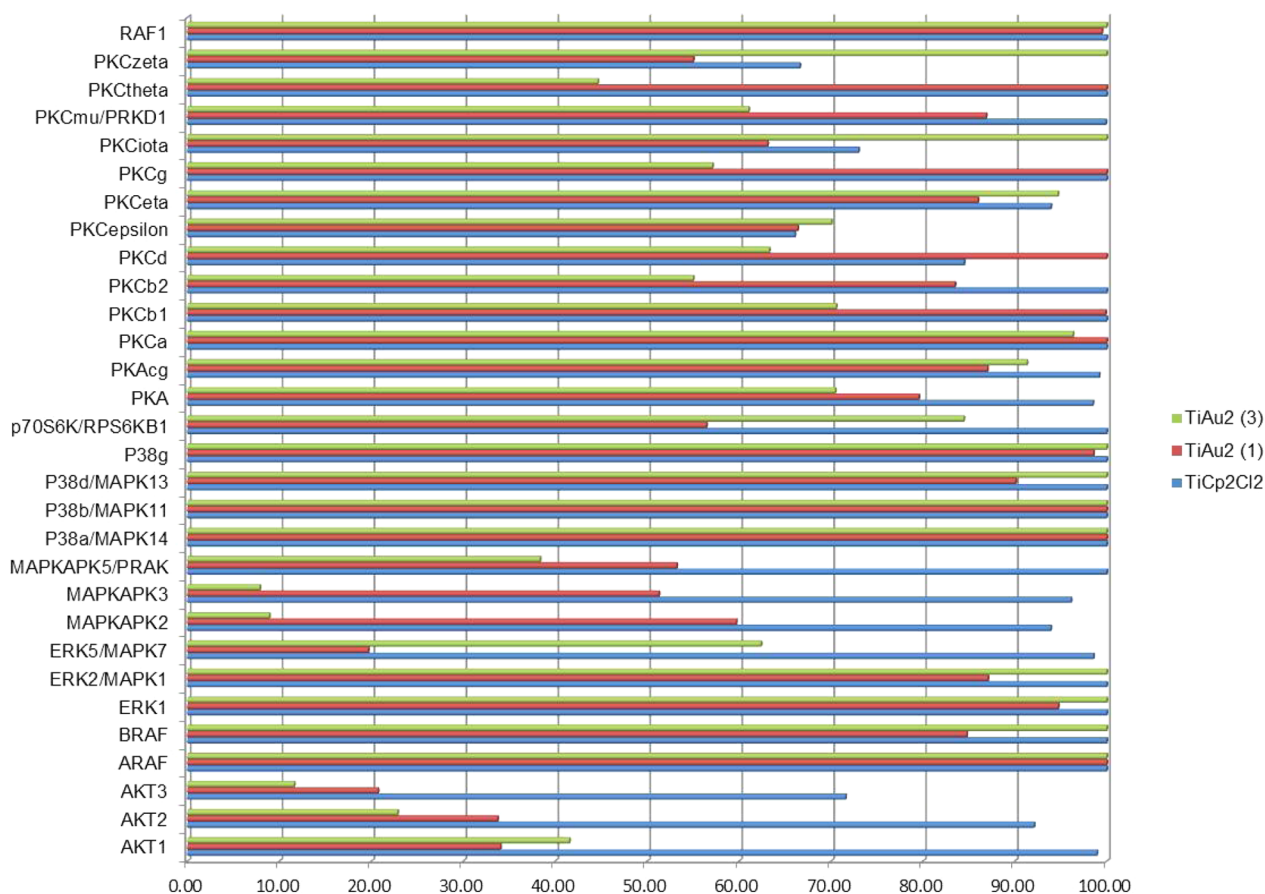


**Figure 7.** Inhibition of enzymatic activity on a panel of 30 kinases (cell-free assay using purified recombinant kinases) by titanocene dichloride [ $\text{Cp}_2\text{TiCl}_2$ ] and heterometallic  $\text{TiAu}_2$  compounds **1** (Chart 2) and **3** (Scheme 1). The y-axis shows the 30 selected protein kinases, while the x-axis displays the enzymatic activity (0 to 100%) in the presence of titanocene dichloride and compounds **1** and **3**.

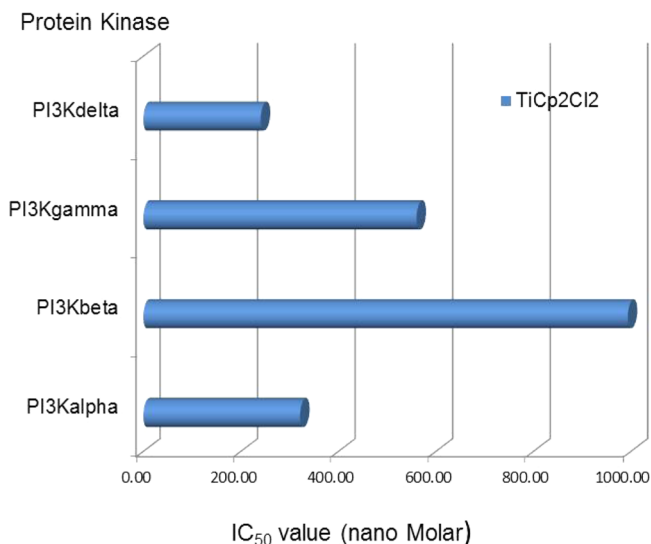


**Figure 8.**  $\text{IC}_{50}$  (nM values) for titanocene dichloride [ $\text{Cp}_2\text{TiCl}_2$ ] against PI3 kinases. Compounds **1** and **3** were poor inhibitors of these lipid PI3 kinases.

**5** do not inhibit the protein kinase mTOR/FRAP1 at concentrations of  $1 \mu\text{M}$ .

There are a very limited number of studies on the inhibition of specific kinases by gold compounds, and to the best of our knowledge there are no reports on studies of this type

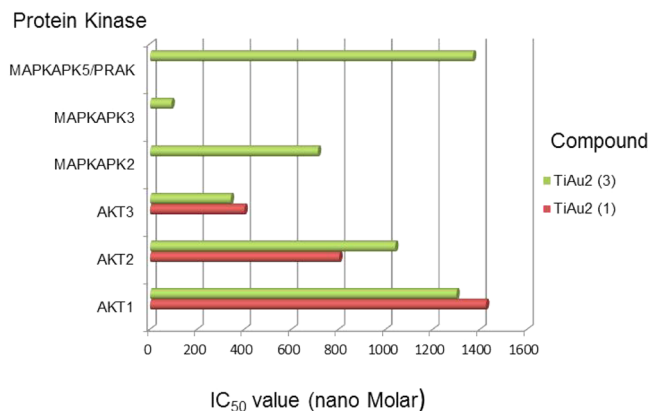


**Figure 9.**  $\text{IC}_{50}$  (nM values) for  $\text{TiAu}_2$  compounds **1** and **3** against selected protein kinases of the AKT and MAPKAPK families. The  $\text{IC}_{50}$  were calculated only for compounds that showed an inhibitory effect of at least 50% when tested at  $10 \mu\text{M}$  concentration (see Figure 7).

performed with titanocene derivatives. A COMPARE analysis on some gold(III) and gold(I) complexes showed some protein kinases as likely biochemical targets.<sup>58</sup> Thus, kinase mTOR is a likely target for Au(I) compounds such as auranofin. For gold(III) derivatives with nitrogen ligands PKC and cyclic protein kinases (CDKs) appear to be plausible targets.<sup>58</sup> More detailed studies were performed for Au(I) compounds aurothioglucose and aurothiomalate, which resulted to be potent inhibitors of PKC $\alpha$ -par6 *in vitro* ( $\text{IC}_{50}$  ca.  $1 \mu\text{M}$ ).<sup>59,60</sup>



We have shown here the inhibitory properties of  $\text{TiAu}_2$  on AKT protein kinases. Importantly, specific  $\text{TiAu}_2$  derivatives such as **3** and **5** also inhibit MAPKAPK2 and MAPKAPK3 with a higher specificity toward MAPKAPK3. Compounds **3** and **5** have an  $\text{IC}_{50}$  value 5 times lower than the most potent MAPKAPK3 kinase inhibitors found among 158 commercially available small molecules that have been screened across 234 human kinases.<sup>61</sup>

To further investigate the ability of these compounds to impair MAPKAPK2/3 activity in cancer cells *in vitro*, we examined the ability of the heterometallic compounds **3** and **5** to inhibit IL6 secretion, which can be activated by MAPKAPK2/3. We found that the compounds significantly reduced secretion of IL-6 in Caki renal cancer cells, which may support the hypothesis that the compounds inhibit activity of MAPKAPK2/3 in these cells.<sup>62</sup> However, other effects such as mitochondrial damage cannot be excluded, and more detailed mechanistic studies are under way.

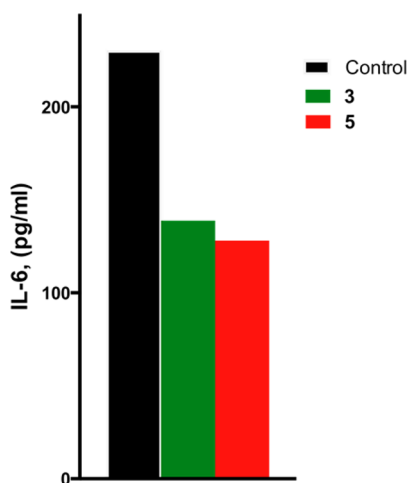


**Figure 10.** Compounds **3** and **5** may affect downstream targets of MAPKAP2/3 in renal cancer cells. Inhibition of IL6 secretion over the course of 6 h in Caki-1 cells treated with compound **3** or **5** (10  $\mu\text{M}$ ). Analysis was done using a capture ELISA approach (human IL-6 ELISA kit).

**2.3. Preliminary Toxicity Data on C57black6 Mice.** The preliminary toxicity testing of compounds **3** and **5** was performed in C57BL/6 female mice 6 to 8 weeks of age (see Experimental Section for details). The lethal dose for compounds **3** and **5** is 15 mg/kg/day, as the mice died within less than 24 h following injection.

The maximum tolerated dose (MTD) was determined by observing the progression of the mice treated at doses below the lethal dose. Body weights, changes in behavior, and signs of distress were recorded. The dose at which neither debilitating effects nor signs of distress were observed was set as the MTD. MTD for compounds **3** and **5** is 10 mg/kg/day. The MTD dose was then confirmed by treating a cohort of three mice per compound and one control group every other day for 14 days with the aforementioned MTD dose. One group of mice was treated with the solvent (negative control). During the trial the mice did not exhibit any notable signs of distress.

Necropsy indicated no notable change in liver or kidney size and appearance. We observed that the spleens of mice treated with compounds **3** and **5** were slightly smaller than control spleens. Enlargement<sup>63</sup> and shrinkage<sup>64–67</sup> of the spleen have

been reported in response to treatment with chemotherapeutics. The compounds can therefore be well tolerated in mice and will be used in subsequent *in vivo* analyses.

## CONCLUSIONS

In conclusion, we have demonstrated that early–late transition metal  $\text{TiAu}_2$  compounds of the type  $[(\eta\text{-C}_5\text{H}_5)_2\text{Ti}\{\text{OC}(\text{O})\text{-RPPH}_2\text{AuCl}\}_2]$  ( $\text{R} = -\text{CH}_2-$  **3**,  $-4\text{-C}_6\text{H}_4-$  **5**) display significant cytotoxicity against human renal cancer cell lines *in vitro*. The convenient high-yield two-step synthesis of **5** starting from commercially available titanocene dichloride is described. The compounds have been significantly more effective than monometallic titanocene dichloride and gold(I)  $[\{\text{HOC}(\text{O})\text{-RPPH}_2\}\text{AuCl}]$  ( $\text{R} = -\text{CH}_2-$  **6**,  $-4\text{-C}_6\text{H}_4-$  **7**) derivatives in renal cancer cell lines, indicating a synergistic effect of the resulting heterometallic species. The activity on renal cancer cell lines (for **5** in the nanomolar range) has been considerably higher than that of cisplatin and highly active Titanocene Y. The cell death induced by the compounds has been studied, indicating apoptosis for compound **5**. The lack of interaction of the compounds with plasmid (pBR322) DNA indicates that other biomolecular targets may be implicated in the cell death pathways. The study of their inhibitory properties on a panel of 35 kinases of oncological interest shows that these compounds inhibit protein kinases of the AKT and MAPKAPK families with a higher selectivity toward MAPKAPK3 ( $\text{IC}_{50}$  **3** = 91 nM,  $\text{IC}_{50}$  **5** = 117 nM). These values make compounds **3** and **5** the most potent MAPKAP3 kinase inhibitors reported so far. In addition, the inhibition of secretion of IL6 in Caki-1 cells observed for **3** and **5** may support the hypothesis that these compounds inhibit activity of MAPKAP2/3 in these cells. Inhibition of MAPKAPK2/3 is therefore likely to mediate in part the antitumor activity of the compounds. We also report here for the first time that titanocene dichloride inhibits PI3 kinases.

This study will undoubtedly help in the design of related compounds (titanocenes and titanocene–gold) with even higher target specificity by rational modification of the ligand scaffolds.

The selectivity of **3** and **5** *in vitro* against renal cancer cell lines when compared to a nontumorigenic human embryonic kidney cell line (HEK-293T) and the favorable preliminary toxicity profile on C57black6 mice indicate that these compounds (especially **5**) can be excellent candidates for further development as potential renal cancer chemotherapeutics.

## EXPERIMENTAL SECTION

**General Procedures.** All compounds involving titanocene fragments were prepared and handled with rigorous exclusion of air and moisture under a nitrogen atmosphere by using standard nitrogen/vacuum manifold and Schlenk techniques. Solvents were purified by use of a PureSolv purification unit from Innovative Technology, Inc. Titanocene dichloride and 4-(diphenylphosphino)benzoic acid were purchased from Aldrich and used without further purification. Diphenylphosphinoacetic acid,<sup>68</sup> complexes **1**,<sup>41</sup> **2**,<sup>44</sup> **3**,<sup>44</sup> and **6**,<sup>45</sup>  $[\text{AuCl}(\text{tht})]$ ,<sup>69</sup> and Titanocene Y<sup>46</sup> were prepared as previously reported. NMR spectra were recorded in a Bruker AV400 ( $^1\text{H}$  NMR at 400 MHz,  $^{13}\text{C}$  NMR at 100.6 MHz, and  $^{31}\text{P}$  NMR at 161.9 MHz). Chemical shifts ( $\delta$ ) are given in ppm using  $\text{CDCl}_3$  as the solvent, unless otherwise stated.  $^1\text{H}$  and  $^{13}\text{C}$  NMR resonances were measured relative to solvent peaks considering tetramethylsilane = 0 ppm, and  $^{31}\text{P}\{^1\text{H}\}$  NMR was externally referenced to  $\text{H}_3\text{PO}_4$  (85%). Coupling constants  $J$  are given in hertz. IR spectra ( $4000\text{--}250\text{ cm}^{-1}$ ) were

recorded on a Nicolet 6700 Fourier transform infrared spectrophotometer on KBr pellets. Elemental analyses were performed by Atlantic Microlab Inc. (US). Mass (MS) spectra (electrospray ionization, ESI) were performed on an Waters XEVO triple quadrupole analyzer and on a Waters Q-ToF Ultima analyzer. The pH was measured in an OAKTON pH conductivity meter in 1:99 DMSO/H<sub>2</sub>O solutions. UV–visible spectra have been recorded using a PerkinElmer Lambda 20 Bio spectrophotometer. X-ray collection was performed at room temperature on a Kappa CCD diffractometer using graphite-monochromated Mo K $\alpha$  radiation ( $\lambda$  = 0.710 73 Å). Electrophoresis experiments were carried out in a Bio-Rad Mini subcell GT horizontal electrophoresis system connected to a Bio-Rad Power Pac 300 power supply. Photographs of the gels were taken with an Alpha Innotech FluorChem 8900 camera. Protein kinase inhibition studies were performed by Reaction Biology Corporation.<sup>70</sup>

**Ph<sub>2</sub>P-4-C<sub>6</sub>H<sub>4</sub>-COONa.** A ethanolic solution of NaOH (1.6 mL, 1 M) was added to a solution of 4-(diphenylphosphino)benzoic acid (0.5 g, 1.63 mmol) in 20 mL of ethanol and stirred for 30 min at room temperature. The ethanol was then removed under reduced pressure to give rise to a white solid, which was washed with diethyl ether (3  $\times$  15 mL) and isolated in 96% yield (0.514 g). <sup>31</sup>P{<sup>1</sup>H} NMR (CDCl<sub>3</sub>):  $\delta$  -6.00. <sup>1</sup>H NMR (CDCl<sub>3</sub>):  $\delta$  7.09 (14H, m). NMR (CDCl<sub>3</sub>):  $\delta$  176.60 (s, C=O), 140.37 (s, 1-C<sub>6</sub>H<sub>4</sub>), 136.85 (d,  $J_{PC}$  = 11.6 Hz, 3-C<sub>6</sub>H<sub>4</sub>), 133.76 (d,  $J_{PC}$  = 20.6 Hz, 1-C<sub>6</sub>H<sub>5</sub>), 132.82 (s, 4-C<sub>6</sub>H<sub>5</sub>), 133.64 (s, 4-C<sub>6</sub>H<sub>4</sub>), 128.60 (m, 2-C<sub>6</sub>H<sub>4</sub>), 3-C<sub>6</sub>H<sub>5</sub>, 2-C<sub>6</sub>H<sub>5</sub>). IR (cm<sup>-1</sup>): 1583 m, 1536 m ( $\nu_{\text{asym}}$  CO<sub>2</sub>), 1377.24 s, 1306 m ( $\nu_{\text{sym}}$  CO<sub>2</sub>).

**[( $\eta$ -C<sub>5</sub>H<sub>5</sub>)<sub>2</sub>Ti{OC(O)-4-C<sub>6</sub>H<sub>4</sub>-PPh<sub>2</sub>}]<sub>2</sub> (4).** Titanocene dichloride (0.095 g, 0.38 mmol) and *p*-Ph<sub>2</sub>P-C<sub>6</sub>H<sub>4</sub>-COONa were dissolved in 6 mL of chloroform, giving rise to a red suspension, which was stirred at room temperature. After 1 h, the suspension became orange. The solvent was removed under vacuum, and the residue dissolved in dichloromethane (8 mL) and extracted to yield a yellow solid (0.249 g, 83%), which was characterized as 4. Anal. Calcd for C<sub>48</sub>H<sub>38</sub>O<sub>4</sub>P<sub>2</sub>Ti (788.64): C, 73.10; H, 4.86. Found: C, 73.35; H, 4.90. <sup>31</sup>P{<sup>1</sup>H} NMR (CDCl<sub>3</sub>):  $\delta$  -5.32. <sup>1</sup>H NMR (CDCl<sub>3</sub>):  $\delta$  7.96 (4H, m), 7.37–7.30 (24H, m), 6.63 (10H, s). <sup>13</sup>C{<sup>1</sup>H} NMR (CDCl<sub>3</sub>):  $\delta$  171.73 (s, C=O), 142.36 (d,  $J_{PC}$  = 13.5 Hz, 1-C<sub>6</sub>H<sub>4</sub>), 136.56 (d,  $J_{PC}$  = 10.8 Hz, 3-C<sub>6</sub>H<sub>4</sub>), 133.87 (d,  $J_{PC}$  = 19.8 Hz, 1-C<sub>6</sub>H<sub>5</sub>), 133.70 (s, 4-C<sub>6</sub>H<sub>5</sub>), 133.32 (d,  $J_{PC}$  = 19.0 Hz, 4-C<sub>6</sub>H<sub>4</sub>), 129.68 (d,  $J_{PC}$  = 6.7 Hz, 2-C<sub>6</sub>H<sub>4</sub>), 129.05 (s, 3-C<sub>6</sub>H<sub>5</sub>), 128.66 (d,  $J_{PC}$  = 7.1 Hz, 2-C<sub>6</sub>H<sub>5</sub>), 118.59 (s, C<sub>5</sub>H<sub>5</sub>). IR (cm<sup>-1</sup>): 3090 m (Cp), 1632 s, 1592 m ( $\nu_{\text{asym}}$  CO<sub>2</sub>), 1338 s, 1305 vs ( $\nu_{\text{sym}}$  CO<sub>2</sub>), 1134 m (Cp), 820 m (Cp). pH of 4 (5  $\times$  10<sup>-5</sup> M in 1:99 DMSO/H<sub>2</sub>O) = 5.32. pH of 2 (5  $\times$  10<sup>-5</sup> M in 1:99 DMSO/H<sub>2</sub>O) = 5.52.

**[( $\eta$ -C<sub>5</sub>H<sub>5</sub>)<sub>2</sub>Ti{OC(O)-4-C<sub>6</sub>H<sub>4</sub>-P(Ph<sub>2</sub>)AuCl}]<sub>2</sub> (5).** Complex 4 (0.213 g, 0.27 mmol) and [AuCl(tht)] (0.175 g, 0.54 mmol) were dissolved in dichloromethane (12 mL) to yield an orange solution, which was stirred for 20 min at room temperature. The dark brown solution was then concentrated to ca. 2, and 20 mL of diethyl ether was added to precipitate complex 5. The heterometallic complex was then isolated by filtration and washed two more times with 20 mL of a mixture of dichloromethane/diethyl ether (1:9). Complex 5 was isolated as a pale yellow solid in 77% yield (0.265 g). Anal. Calcd for C<sub>48</sub>H<sub>38</sub>Au<sub>2</sub>Cl<sub>2</sub>O<sub>4</sub>P<sub>2</sub>Ti (1253.48): C, 45.99; H, 3.06. Found: C, 45.76; H, 3.31. <sup>31</sup>P{<sup>1</sup>H} NMR (CDCl<sub>3</sub>):  $\delta$  32.99. <sup>1</sup>H NMR (CDCl<sub>3</sub>):  $\delta$  8.08 (4H, m), 7.55 (24H, m), 6.66 (10H, s). <sup>13</sup>C{<sup>1</sup>H} NMR (CDCl<sub>3</sub>):  $\delta$  170.35 (s, C=O), 136.83 (d,  $J_{PC}$  = 2.4 Hz, 1-C<sub>6</sub>H<sub>4</sub>), 134.22 (d,  $J_{PC}$  = 13.8 Hz, 3-C<sub>6</sub>H<sub>4</sub>), 133.96 (d,  $J_{PC}$  = 13.9 Hz, 1-C<sub>6</sub>H<sub>5</sub>), 132.80 (d,  $J_{PC}$  = 60.3 Hz, 4-C<sub>6</sub>H<sub>5</sub>), 132.39 (d,  $J_{PC}$  = 2.5 Hz, 4-C<sub>6</sub>H<sub>4</sub>), 130.26 (d,  $J_{PC}$  = 12.0 Hz, 2-C<sub>6</sub>H<sub>4</sub>), 129.46 (d,  $J_{PC}$  = 12.0 Hz, 2-C<sub>6</sub>H<sub>5</sub>), 128.13 (d,  $J_{PC}$  = 62.5 Hz, 3-C<sub>6</sub>H<sub>5</sub>), 119.0 (s, C<sub>5</sub>H<sub>5</sub>). IR (cm<sup>-1</sup>): 3180 w (Cp), 1643 vs ( $\nu_{\text{asym}}$  CO<sub>2</sub>), 1558 s (Cp), 1330s, 1292 vs ( $\nu_{\text{sym}}$  CO<sub>2</sub>), 1100 m (Cp), 823 s (Cp), 328 ms ( $\nu$  AuCl). pH of 5 (5  $\times$  10<sup>-5</sup> M in 1:99 DMSO/H<sub>2</sub>O) = 5.10. For comparison, the pH of previously described compound 3<sup>44</sup> (5  $\times$  10<sup>-5</sup> M in 1:99 DMSO/H<sub>2</sub>O) = 6.12.

**[AuCl(P(Ph<sub>2</sub>)-4-C<sub>6</sub>H<sub>4</sub>-COOH)] (7).** 4-(Diphenylphosphino)benzoic acid (0.144 g, 0.47 mmol) and [AuCl(tht)] (0.151 g, 0.47 mmol) were dissolved in dichloromethane (10 mL) and stirred for 30 min at room temperature. The solvent was removed under reduced pressure to yield a white crude, which was washed with diethyl ether (3  $\times$  10 mL).

Complex 7 was isolated as a white solid in 66% yield (0.168 g). Anal. Calcd for C<sub>19</sub>H<sub>15</sub>AuClO<sub>2</sub>P (538.71): C, 42.36; H, 2.81. Found: C, 42.54; H, 2.98. <sup>31</sup>P{<sup>1</sup>H} NMR (CDCl<sub>3</sub>):  $\delta$  33.22. <sup>1</sup>H NMR (CDCl<sub>3</sub>):  $\delta$  11.17 (1H, s), 8.19 (2H, dd, <sup>3</sup> $J_{HH}$  = 8.3 Hz, <sup>4</sup> $J_{HH}$  = 1.9 Hz), 7.57 (13H, m). <sup>13</sup>C{<sup>1</sup>H} NMR (CDCl<sub>3</sub>):  $\delta$  169.89 (s, C=O), 135.53 (d,  $J_{PC}$  = 59.6 Hz, 4-C<sub>6</sub>H<sub>4</sub>), 134.29 (d,  $J_{PC}$  = 13.9 Hz, 2'-C<sub>6</sub>H<sub>4</sub>), 134.07 (d,  $J_{PC}$  = 13.9 Hz, 2-C<sub>6</sub>H<sub>5</sub>), 132.43 (d,  $J_{PC}$  = 2.5 Hz, 1-C<sub>6</sub>H<sub>5</sub>), 132.19 (s, 4'-C<sub>6</sub>H<sub>4</sub>), 130.57 (d,  $J_{PC}$  = 11.9 Hz, 3-C<sub>6</sub>H<sub>4</sub>), 129.50 (d,  $J_{PC}$  = 12.0 Hz, 3'-C<sub>6</sub>H<sub>5</sub>), 127.77 (d,  $J_{PC}$  = 62.6 Hz, 1'-C<sub>6</sub>H<sub>5</sub>). IR (cm<sup>-1</sup>): 1682 vs ( $\nu_{\text{asym}}$  CO<sub>2</sub>), 1377 s ( $\nu_{\text{sym}}$  CO<sub>2</sub>), 342 ms ( $\nu$  AuCl).

**X-ray Crystallography.** A single crystal of 3 (see details in Table S1 in the SI) was mounted on a glass fiber in a random orientation. Data collection was performed at RT on a Kappa CCD diffractometer using graphite-monochromated Mo K $\alpha$  radiation ( $\lambda$  = 0.710 73 Å). Space group assignments were based on systematic absences, E statistics, and successful refinement of the structures. The structure was solved by direct methods with the aid of successive difference Fourier maps and was refined using the SHELXTL 6.1 software package. All non-hydrogen atoms were refined anisotropically. Hydrogen atoms were assigned to ideal positions and refined using a riding model. Details of the crystallographic data are given in Table S1 (SI). These data can be obtained free of charge from the Cambridge Crystallographic Data Center via [www.ccdc.cam.ac.uk/data\\_request/cif](http://www.ccdc.cam.ac.uk/data_request/cif) (CCDC 1008332) or in the SI. Crystals of 3 (yellow prisms with approximate dimensions 0.25  $\times$  0.23  $\times$  0.22 mm) were obtained from a solution of 3 in CH<sub>2</sub>Cl<sub>2</sub> by slow diffusion of Et<sub>2</sub>O at RT.

**Cell Culture.** Human renal cell carcinoma lines A498, Caki-1, and UO31, as well as the human prostate carcinoma cell lines DU145 and PC3, were newly obtained for these studies from the American Type Culture Collection (ATCC) (Manassas, VA, USA) and cultured in Roswell Park Memorial Institute (RPMI-1640) (Mediatech Inc., Manassas, VA, USA) media containing 10% fetal bovine serum (FBS, Life Technologies, Grand Island, NY, USA), 1% minimum essential media (MEM) nonessential amino acids (NEAA, Mediatech), and 1% penicillin–streptomycin (PenStrep, Mediatech). HEK-293 cells were newly purchased from ATCC and maintained in Dulbecco's modified Eagle's medium (DMEM) (Mediatech) supplemented with 10% FBS, 1% NEAA, and 1% PenStrep. All cells were cultured at 37 °C and 5% CO<sub>2</sub> in a humidified incubator.

**Cell Viability Assay.** Cells were seeded at a concentration of 5000 cells/90  $\mu$ L per well of either RPMI or DMEM without phenol red and without antibiotics, supplemented with 10% FBS and 2 mM L-glutamine into tissue culture grade 96-well flat bottom microplates (Thermo Scientific BioLite microwell plates, Fisher Scientific, Waltham, MA, USA) and grown for 24 h at 37 °C in a humidified incubator. Afterward, the intermediate dilutions of the compounds were added to the wells (10  $\mu$ L) to obtain a final concentration ranging from 0.1 to 200  $\mu$ M, and the cells were incubated for 24 or 72 h. Following 24 or 72 h drug exposure, 50  $\mu$ L per well of 2,3-bis(2-methoxy-4-nitro-5-sulphophenyl)-2H-tetrazolium-5-carboxanilide (XTT) (Roche Diagnostics, Indianapolis, IN, USA) labeling mixture was added to the cells at a final concentration of 0.3 mg/mL and incubated for 4 h at 37 °C in a humidified incubator. The optical absorbance of each well (96-well plates) was quantified using EnVision multilabel plate readers (PerkinElmer, Waltham, MA, USA) at 450 nm wavelength. The percentage of surviving cells was calculated from the ratio of absorbance of treated to untreated cells. The IC<sub>50</sub> value was calculated as the concentration reducing the proliferation of the cells by 50% and is presented as a mean ( $\pm$ SE) of at least two independent experiments each with triplicates.

**Annexin V/PI Assay.** Confluent Caki-1 cells were treated with either 10  $\mu$ M 3 or 5, 0.1% DMSO, or 5  $\mu$ M staurosporine for 6 h (Figure 4) or for 1 h, 12 h, or 24 h (S34–S36). After incubation, cells were trypsinized with 0.25% trypsin without EDTA (ethylenediaminetetraacetic acid, Life Technologies) and stained for extracellular phosphatidylserine expression using FITC conjugated annexin V to label early apoptotic cells and costained with propidium iodide to identify necrotic cells according to the manufacturer's instructions for the dyes (BD Biosciences, San Jose, CA, USA). Stained cells were

analyzed by flow cytometry using Accuri C6 (BD Biosciences) and Accuri C6 analyzing software.

**Interaction of Compounds 3 and 5–7, Titanocene Dichloride, and Cisplatin with Plasmid (pBR322) DNA by Electrophoresis (Mobility Shift Assay).** Aliquots of 10  $\mu$ L of plasmid (pBR322) DNA (20  $\mu$ g/mL) in buffer (5 mM Tris/HCl, 50 mM NaClO<sub>4</sub>, pH = 7.39) were incubated with different concentrations of the compounds (3, 5–7, and titanocene dichloride) (in the range 0.25 and 4.0 metal complex/DNAbp (bp = base pairs)) at 37 °C for 20 h in the dark. Samples of free DNA and cisplatin-DNA were prepared as controls. After the incubation period, the samples were loaded onto the 1% agarose gel. The samples were separated by electrophoresis for 1.5 h at 80 V in Tris-acetate/EDTA buffer. Afterward, the gel was stained for 30 min with a solution of GelRed nucleic acid stain.

**Kinase Inhibition Studies.** *In vitro* profiling of 34 selected member kinase panel was performed at Reaction Biology Corporation using the “HotSpot” assay platform. Briefly, specific kinase/substrate pairs along with required cofactors<sup>70</sup> were prepared in reaction buffer: 20 mM Hepes pH 7.5, 10 mM MgCl<sub>2</sub>, 1 mM EGTA (ethylene glycol tetracetic acid), 0.02% Brij35, 0.02 mg/mL BSA (bovine serum albumin), 0.1 mM Na<sub>3</sub>VO<sub>4</sub>, 2 mM DTT (dithiothreitol), 1% DMSO. Compounds were delivered into the reaction, followed ~20 min later by addition of a mixture of ATP (Sigma) and <sup>33</sup>P-ATP (PerkinElmer) to a final concentration 10  $\mu$ M. Reactions were carried out at 25 °C for 120 min, followed by spotting of the reactions onto P81 ion exchange filter paper (Whatman). Unbound phosphate was removed by extensive washing of filters in 0.75% phosphoric acid. After subtraction of background derived from control reactions containing inactive enzyme, kinase activity data were expressed as the percent remaining kinase activity in test samples compared to vehicle (dimethyl sulfoxide) reactions. IC<sub>50</sub> values and curve fits were obtained using Prism (GraphPad Software, La Jolla, CA, USA).

**Concentrations of Cytokine IL-6.** The concentrations of cytokine IL-6 secreted were determined from cell supernatants collected after 6 h of incubation with compound 3 or 5 by an ELISA kit (human IL-6 ELISA kit) according to the manufacturer's instructions (Thermo Fisher Scientific, Rockford, IL, USA). Optical density was measured using a microplate reader (PerkinElmer) at 450 nm wavelength. Concentrations of the cytokine were determined by interpolation from the standard curves using Prism (GraphPad Software).

**Determination of Lethal and Maximum Tolerated Doses (LD and MTD) in Mice.** The preliminary toxicity testing of compounds 3 and 5 was performed in C57BL/6 female mice 6 to 8 weeks of age, maintained in accordance with institutional guidelines at the University of Hawaii Cancer Center (UHCC) governing the care of laboratory animals (IACUC number: A3423-01). To determine the lethal dose, mice were treated for five consecutive days at dosages ranging from 5 to 20 mg/kg/day. We used one mouse per dose. Mice were weighed every 48 h and sacrificed 24 h after the last dose. The compounds were administered in a solution of 0.5% DMSO and 99.5% normal saline (0.9% NaCl) (G-Biosciences, St. Louis, MO, USA) once daily by subcutaneous injection. In order to determine the maximum tolerated dose, the animals were monitored by trained individuals for pain and distress as appropriate for the species, condition, and procedure at the UH vivarium by the veterinarian staff and person doing the *in vivo* studies (B.T.E.). The maximum tolerated dose was determined by observing the progression of the mice treated at doses below the lethal dose. Body weights, changes in behavior, and signs of distress were recorded. The dose at which neither debilitating effects nor signs of distress was observed and set as the MTD. More specifically the signs of distress monitored were (1) decreased food and water consumption; (2) weight loss (more than 20% loss in body weight or dropping to or below 18 g) was consistent with significant distress and mice exhibiting such weight loss were euthanized; (3) abnormal posture/positioning (e.g., head-pressing, hunched back); (4) unkempt appearance (erected, matted, or dull haircoat); (5) self-mutilation, gnawing at limbs; (6) excessive self-imposed isolation/hiding. The MTD dose was then confirmed by treating a cohort of

three mice per compound and one control group every other day for 14 days with the aforementioned MTD dose. One group of mice was treated with the solvent (negative control). During the trial the mice did not exhibit any notable signs of distress.

## ■ ASSOCIATED CONTENT

### ■ Supporting Information

Table with the crystal data and structure refinement for complex 3. CIF file for the X-ray crystal structure of compound 3. Ortep view of the crystal structure of 3 including labeled carbon atoms. <sup>1</sup>H, <sup>31</sup>P{<sup>1</sup>H}, and <sup>13</sup>C{<sup>1</sup>H} NMR spectra of new compounds 4, 5, and 7. Stability of compounds 3 and 5 in *d*<sub>6</sub>-DMSO solution and in *d*<sub>6</sub>-DMSO/D<sub>2</sub>O (50:50) over time assessed by <sup>31</sup>P{<sup>1</sup>H} and <sup>1</sup>H NMR spectroscopy. UV–vis spectra of compounds 3 and 5 in CH<sub>2</sub>Cl<sub>2</sub>, DMSO, and (1% DMSO) PBS solution over time. Mass spectra of 3 and 5 in (1% DMSO) PBS solution over time. Cell death experiments (annexin V/PI assay) for compound 3 at 1 and 12 h and compound 5 at 12 and 24 h. This material is available free of charge via the Internet at <http://pubs.acs.org>.

## ■ AUTHOR INFORMATION

### Corresponding Authors

\*Phone: 1-808-564-5843. Fax: 1-808-586-2970. E-mail: [jramos@cc.hawaii.edu](mailto:jramos@cc.hawaii.edu).

\*Phone: 1-7189515000, x2833. Fax: 1-718-951-4607. E-mail: [mariacontel@brooklyn.cuny.edu](mailto:mariacontel@brooklyn.cuny.edu).

### Present Address

<sup>†</sup>Moores Cancer Center, University of California, San Diego, La Jolla, California 92093, United States.

### Author Contributions

The manuscript was written through contributions of all authors. All authors have given approval to the final version of the manuscript.

### Notes

The authors declare no competing financial interest.

## ■ ACKNOWLEDGMENTS

We thank the National Cancer Institute (NCI) for grant 1SC1CA182844 (M.C.) and the National General Medical Sciences Institute (NGMSI) for grant RO1GM088266-A1 (J.W.R.). M.C. is very grateful to Mr. and Mrs. Leonard and Claire Tow and the Tow Foundation for a travel fellowship to perform some experiments at the University of Hawaii Cancer Center. We thank Dr. Monica Carreira for her assistance with the synthesis of compound 1. We thank Dr. Chris Farrar (University of Hawaii Cancer Center) for assistance with the flow cytometry experiments and Prof. Wei Jia and Dr. Guoxiang Xie (University of Hawaii Cancer Center) for performing the MS spectra of compounds 3 and 5.

## ■ REFERENCES

- (1) Thayer, A. M. Platinum drugs take their roll. *Chem. Eng. News* **2010**, 88 (26), 24–28.
- (2) Kelland, L. The resurgence of platinum-based cancer chemotherapy. *Nat. Rev. Cancer* **2007**, 7, 573–584.
- (3) Alessio, E. *Bioinorganic Medicinal Chemistry*; Wiley-VCH: Weinheim, Germany, 2011.
- (4) Noffke, A. L.; Habtemarian, A.; Pizarro, A. M.; Sadler, P. J. Designing organometallic compounds for catalysis and therapy. *Chem. Commun.* **2012**, 48, 5219–5246.
- (5) Aris, S. M.; Farrell, N. P. Towards antitumor active trans-platinum compounds. *Eur. J. Inorg. Chem.* **2009**, 1293–1302.



- (6) Berners-Price, S. J.; Filipovska, A. Gold compounds as therapeutic agents for human diseases. *Metallomics* **2011**, No. 41, 279–304.
- (7) Komeda, S.; Casini, A. Next-generation anticancer metalldrugs. *Curr. Top. Med. Chem.* **2012**, 12, 219–223.
- (8) Bergamo, A.; Gaiddon, C.; Schellens, J. H. M.; Beijnen, J. H.; Sava, G. Approaching tumour therapy beyond platinum drugs: status of the art and perspectives of ruthenium drug candidates. *J. Inorg. Biochem.* **2012**, 106, 90–99.
- (9) Harding, M. M.; Mokdsi, G. Antitumour metallocenes: structure-activity studies and interactions with biomolecules. *Curr. Med. Chem.* **2000**, 7, 1289 and references therein.
- (10) Köpf-Maier, P.; Köpf, H. Titanocene dichloride - the first metallocene with cancerostatic activity. *Angew. Chem., Int. Ed. Engl.* **1979**, 18, 477.
- (11) Berdel, W. E.; Schmoll, H. J.; Scheulen, M. E.; Korfel, A.; Knoche, M. F.; Harstrick, A.; Bach, F.; Sa, G. Phase I clinical trial of titanocene dichloride in adults with advanced solid tumors. *J. Cancer Res. Clin. Oncol.* **1994**, 120 (Suppl), R172.
- (12) Abeyasinghe, P. M.; Harding, M. M. Antitumor bis-(cyclopentadienyl) metal complexes: titanocene and molybdocene dichloride and derivatives. *Dalton Trans.* **2007**, 3474 and references therein.
- (13) Olszewski, U.; Hamilton, G. Mechanisms of cytotoxicity of anticancer titanocenes. *Anti-Cancer Agents Med. Chem.* **2010**, 10, 320 and references therein.
- (14) Lummen, G.; Sperling, H.; Lubolt, H.; Otto, T.; Rubben, H. Phase II trial of titanocene dichloride in advanced renal-cell carcinoma. *Cancer Chemother. Pharmacol.* **1998**, 42, 415.
- (15) Kroger, N.; Kleeberg, U. R.; Mross, K.; Edler, L.; Sab, G.; Hossfeld, D. Phase II clinical trial of titanocene dichloride in patients with metastatic breast cancer. *Onkologie* **2000**, 23, 288.
- (16) Strohfeldt, K.; Tacke, M. Biorganometallic fulvene-derived titanocene anti-cancer drugs. *Chem. Soc. Rev.* **2008**, 37, 1174–1187.
- (17) Recent selected example: Olszewski, U.; Deally, A.; Tacke, M.; Hamilton, G. Alterations of phosphoproteins in NCI-H526 small cell lung cancer cells involved in cytotoxicity of cisplatin and titanocene Y. *Neoplasia* **2012**, 14, 813–822 and references therein.
- (18) Beckhove, P.; Oberschmidt, O.; Hanauske, A. R.; Pampillón, C.; Schirmacher, V.; Sweeney, N. J.; Strohfeldt, K.; Tacke, M. Antitumor activity of titanocene Y against freshly explanted human breast tumor cells and in xenografted MCF-7 tumors in mice. *Anti-Cancer Drugs* **2007**, 18, 311.
- (19) Bannon, J. H.; Fitchner, I.; O'Neill, A.; Pampillón, C.; Sweeney, N. J.; Strohfeldt, K.; Watson, R. W.; Tacke, M.; Mc Gee, M. M. Substituted titanocenes induce caspase-dependent apoptosis in human epidermoid carcinoma cells in vitro and exhibit antitumor activity in vivo. *Br. J. Cancer* **2007**, 97, 1234.
- (20) Fichtner, I.; Pampillón, C.; Sweeney, N. J.; Strohfeldt, K.; Tacke, M. Anti-tumor activity of titanocene Y in xenografted Caki-1 tumors in mice. *Anti-Cancer Drugs* **2006**, 17, 333.
- (21) Fichtner, I.; Behrens, D.; Claffey, J.; Deally, A.; Gleeson, B.; Patil, S.; Weber, H.; Tacke, M. The antiangiogenic and antitumoral activity of Titanocene Y\* in vivo. *Lett. Drug Des. Discovery* **2011**, 8, 302–307.
- (22) Walther, W.; Fichtner, I.; Deally, A.; Hogan, M.; Tacke, M. The activity of Titanocene T against xenografted caki-1 tumors. *Lett. Drug Des. Discovery* **2013**, 10, 375–381.
- (23) Bertrand, B.; Casini, A. A golden future in medicinal inorganic chemistry: the promise of anticancer organometallic gold complexes. *Dalton Trans.* **2014**, 43, 4209–4219.
- (24) Nobili, S.; Mini, E.; Landini, I.; Gabbiani, C.; Casini, A.; Messori, L. Gold compounds as anticancer agents: chemistry, cellular pharmacology, and preclinical studies. *Med. Res. Rev.* **2010**, 30, 550–580.
- (25) Casini, A.; Hartinger, C.; Gabbiani, C.; Mini, E.; Dyson, P. J.; Keppler, B. K.; Messori, L. Gold(III) compounds as anticancer agents: relevance of gold-protein interactions for their mechanism of action. *J. Inorg. Biochem.* **2008**, 102, 564–575.
- (26) Schuh, E.; Pfluger, C.; Citta, A.; Folda, A.; Rigobello, M. P.; Bindoli, A.; Casini, A.; Mohr, F. Gold(I) carbene complexes causing thioredoxin 1 and thioredoxin 2 oxidation as potential anticancer agents. *J. Med. Chem.* **2012**, 55, 5518–5528 and references therein.
- (27) Berners-Price, S. J.; Filipovska, A. Gold compounds as therapeutic agents for human diseases. *Metallomics* **2011**, 3, 863–873.
- (28) Dalla Via, L.; Nardon, C.; Fregona, D. Targeting the ubiquitin-proteasome pathway with inorganic compounds to fight cancer: a challenge for the future. *Future Med. Chem.* **2012**, 4, 525–543.
- (29) Casini, A.; Kelter, G.; Gabbiani, C.; Cinellu, M. A.; Minghetti, G.; Fregona, D.; Fiebig, H.-H.; Messori, L. Chemistry, antiproliferative properties, tumor selectivity, and molecular mechanisms of novel gold(III) compounds for cancer treatment: a systematic study. *J. Biol. Inorg. Chem.* **2009**, 14, 1139–1149.
- (30) Magherini, F.; Modesti, A.; Bini, L.; Puglia, M.; Landini, I.; Nobili, S.; Mini, E.; Cinellu, M. A.; Gabbiani, C.; Messori, L. Exploring the biochemical mechanisms of cytotoxic gold compounds: a proteomic study. *J. Biol. Inorg. Chem.* **2010**, 15, 573–582.
- (31) Zhu, Y.; Cameron, B. R.; Mosi, R.; Anastassov, V.; Cox, J.; Qin, L.; Santucci, Z.; Metz, M.; Skerlj, R. T.; Fricker, S. P. Inhibition of the cathepsin cysteine proteases B and K by square-planar cycloaurated gold(III) compounds and investigation of their anti-cancer activity. *J. Inorg. Biochem.* **2011**, 105, 754–762.
- (32) Erdogan, E.; Lamark, T.; Stallings-mann, M.; Jamieson, L.; Pellecchia, M.; Thompson, E. A.; Johansen, T.; Fields, A. P. Aurothiomalate inhibits transformed growth by targeting the PB1 domain of protein kinase C $\alpha$ . *J. Biol. Chem.* **2006**, 281, 28450–28459.
- (33) Stallings-Mann, M.; Jamieson, L.; Regala, R. P.; Weems, C.; Murray, N. R.; Fields, A. P. A novel small molecule inhibitor of protein kinase C $\alpha$  blocks transformed growth of non-small-cell lung cancer cell. *Cancer Res.* **2006**, 66, 1767–1764.
- (34) Jeon, K. I.; Biun, M. S.; Jue, D. M. Gold compound auranofin inhibits I $\kappa$ B kinase (IKK) by modifying Cys-179 of IKK $\beta$  subunit. *Exp. Mol. Med.* **2003**, 35, 61–66.
- (35) Serratrice, M.; Edafe, F.; Mendes, F.; Scopelliti, R.; Zakeeruddin, S. M.; Gratzel, M.; Santos, I.; Cinellu, M. A.; Casini, A. Cytotoxic gold compounds: synthesis, biological characterization and investigation on their inhibition properties of the zinc finger protein PARP-1. *Dalton Trans.* **2012**, 41, 3287–3293.
- (36) Mendes, F.; Groessel, M.; Nazarov, A. A.; Tsybin, Y. O.; Sava, G.; Santos, I.; Dyson, P. J.; Casini, A. Metal-based inhibition of poly(ADP-ribose)polymerase—the guardian angel of DNA. *J. Med. Chem.* **2011**, 54, 2196–2206.
- (37) Lease, N.; Vasilevski, V.; Carreira, M.; de Almeida, A.; Sanaú, M.; Hirva, P.; Casini, A.; Contel, M. Potential anticancer heterometallic Fe–Au and Fe–Pd agents: initial mechanistic insights. *J. Med. Chem.* **2013**, 56, 5806–5818.
- (38) Cooper, B. G.; Napoline, J. W.; Thomas, C. Catalytic applications of early/late heterobimetallics. *Catal. Rev. Sci. Eng.* **2012**, 54, 1–40.
- (39) Pelletier, F.; Comte, V.; Massard, A.; Wenzel, M.; Toulot, S.; Richard, P.; Picquet, M.; Le Gendre, P.; Zava, O.; Edafe, F.; Casini, A.; Dyson, P. J. Development of bimetallic titanocene-ruthenium-arene complexes as anticancer agents: relationships between structural and biological properties. *J. Med. Chem.* **2010**, 53, 6923–6933.
- (40) Wenzel, M.; Bertrand, B.; Eymin, M.-J.; Comte, V.; Harvey, J. A.; Richard, P.; Groessel, M.; Zava, O.; Amrouche, H.; Harvey, P. D.; Le Gendre, P.; Picquet, M.; Casini, A. Multinuclear cytotoxic metalldrugs: physicochemical characterization and biological properties of novel heteronuclear gold-titanium complexes. *Inorg. Chem.* **2011**, 50, 9472–9480.
- (41) González-Pantoja, J. F.; Stern, M.; Jarzecki, A. A.; Royo, E.; Robles-Escajeda, E.; Varela-Ramirez, A.; Aguilera, R. J.; Contel, M. Titanocene-phosphine derivatives as precursors to cytotoxic heterometallic TiAu $_2$  and TiM (M = Pd, Pt) compounds. studies of their interactions with DNA. *Inorg. Chem.* **2011**, 50, 11099–11110.
- (42) (a) Chen, X.; Zhou, L. The hydrolysis chemistry of anticancer drug titanocene dichloride: an insight from theoretical study. *J. Mol. Struct.* **2010**, 940, 45–49. (b) Olszewski, U.; Hamilton, G.



Mechanisms of cytotoxicity of anticancer titanocenes. *Anti-Cancer Agents Med. Chem.* **2010**, *10*, 302–311 and references therein.

(43) (a) Buettner, K. M.; Snoeberger, R. C., III; Batista, V. S.; Valentine, A. M. Pharmaceutical formulation affects titanocene transferring interactions. *Dalton Trans.* **2011**, *40*, 9580–9588. (b) Parker Siburt, C. J. P.; Lin, E. M.; Brandt, S. J.; Tinoco, A. D.; Valentine, A. M.; Crumbliss, A. L. Redox potentials of Ti(IV) and Fe(III) complexes provide insights into titanium biodistribution mechanisms. *J. Inorg. Biochem.* **2010**, *104*, 1006–1009.

(44) Edwards, D. A.; Mahon, M. F.; Paget, T. J. Diphenylphosphinoacetate, nicotinate and thiphenoxycetate as bridging ligands in heterometallic complexes involving bis( $\eta$ -cyclopentadienyl)titanium-(IV) and group 10 or 11 metal chlorides. Crystal structures of  $[(\eta\text{-C}_5\text{H}_5)_2\text{Ti}\{\text{OC}(\text{O})\text{CH}_2\text{PPh}_2\}_2]$  and  $[(\eta\text{-C}_5\text{H}_5)_2\text{Ti}\{\text{OC}(\text{O})\text{CH}_2\text{PPh}_2\}_2\text{PdCl}_2]$ . *Polyhedron* **2000**, *19*, 757–764.

(45) Edwards, D. A.; Mahon, M. F.; Paget, T. J. Some metal complexes containing diphenylphosphinoacetic acid as a P-bonded neutral ligand. Crystal structures of  $[\text{AuCl}(\text{Ph}_2\text{PCH}_2\text{CO}_2\text{H})]$  and  $\text{trans-}[\text{PdCl}_2(\text{Ph}_2\text{PCH}_2\text{CO}_2\text{H})_2] \cdot 0.33\text{H}_2\text{O} \cdot 0.33\text{C}_2\text{H}_5\text{OH}$ . *Polyhedron* **1998**, *17*, 4121–4130.

(46) Sweeney, N. J.; Mendoza, O.; Muller-Bunz, H.; Pampillon, C.; Rehmann, F.-J. K.; Strohsfeldt, K.; Tacke, M. Novel benzyl substituted titanocene anti-cancer drugs. *J. Organomet. Chem.* **2005**, *690*, 4537–4544.

(47) Shaik, N.; Martínez, A.; Augustin, I.; Giovinozzo, H.; Varela, A.; Aguilera, R.; Sanaú, M.; Contel, M. Synthesis of apoptosis-inducing iminophosphorane organogold(III) complexes and study of their interactions with biomolecular targets. *Inorg. Chem.* **2009**, *48*, 1577–1587.

(48) Elie, B. T.; Levine, C.; Ubarretxena-Belandia, I.; Varela-Ramirez, A.; Aguilera, R. J.; Contel, M. Water soluble phosphane-gold(I) complexes. Applications as recyclable catalysts in a three-component coupling reaction and as anticancer and antimicrobial agents. *Eur. J. Inorg. Chem.* **2009**, 3421–3430.

(49) Dabrowiak, J. C. *Metals in Medicine*; John Wiley and Sons, Ltd: Chichester, UK, 2009; Chapter 4, pp 109–114.

(50) Liu, H.-K.; Sadler, P. Metal complexes as DNA intercalators. *Acc. Chem. Res.* **2011**, *44*, 349–359.

(51) Kopf-Maier, P.; Wagner, W.; Liss, E. Induction of cell arrest at G1/S and G2 after treatment of Ehrlich ascites tumor cells with metallocene dichlorides. *J. Cancer Res. Clin. Oncol.* **1982**, *103*, 145–164.

(52) Christodoulou, C. V.; Eliopulos, A. G.; Young, L. S.; Hodgkins, L.; Ferry, D. R.; Kerr, D. J. Anti-proliferative activity and mechanism of action of titanocene dichloride. *Br. J. Cancer* **1998**, *77*, 2088–2097.

(53) Rivera, M.; Gabano, E.; Baracco, S.; Osella, D. Eletrochemical evaluation of the interaction between antitumoral titanocene dichloride and biomolecules. *Inorg. Chim. Acta* **2009**, *362*, 1303–1306 and references therein.

(54) Lally, G.; Deally, A.; Hackenberg, F.; Quinn, S. J.; Tacke, M. Titanocene Y – transport and targeting of an anticancer drug candidate. *Lett. Drug Des. Discovery* **2013**, *10*, 675–682.

(55) Fox, K. *Drug-DNA Interaction Protocols Methods in Molecular Biology*; Humana Press Inc: Totowa, NJ, 1997.

(56) Feng, L.; Geisselbrecht, Y.; Blanck, S.; Wilbuer, A.; Atilla-Gokcumen, G. E.; Filippakopoulos, P.; Kraling, K.; Celik, M. A.; Harms, K.; Maksimoska, J.; Marmorstein, R.; Frenking, G.; Knapp, S.; Essen, L.-O.; Meggers, E. Structurally sophisticated octahedral metal complexes as highly selective protein kinase inhibitors. *J. Am. Chem. Soc.* **2011**, *133*, 5976–5986.

(57) Meggers, E. From conventional to unusual enzyme inhibitor scaffolds: The quest for target specificity. *Angew. Chem., Int. Ed.* **2011**, *50*, 2442–2448.

(58) Mulcahy, S. P.; Meggers, E. Organometallics as structural scaffolds for enzyme inhibitor design. *Top. Organomet. Chem.* **2010**, *32*, 141–153.

(59) Casini, A.; Kelter, G.; Gabbiani, C.; Cinellu, M. A.; Minghetti, G.; Fregona, D.; Fiebig, H.-H.; Messori, L. Chemistry, antiproliferative properties, tumor selectivity, and molecular mechanisms of novel

gold(III) compounds for cancer treatment: a systematic study. *J. Biol. Inorg. Chem.* **2009**, *14*, 1139.

(60) Erdogan, E.; Lamark, T.; Stallings-mann, M.; Jamieson, L.; Pellecchia, M.; Thompson, E. A.; Johansen, T.; Fields, A. P. Aurothiomalate inhibits transformed growth by targeting the PB1 domain of protein kinase C $\alpha$ . *J. Biol. Chem.* **2006**, *281*, 28450–28459.

(61) Stallings-Mann, M.; Jamieson, L.; Regala, R. P.; Weems, C.; Murray, N. R.; Fields, A. P. A novel small molecule inhibitor of protein kinase C $\alpha$  blocks transformed growth of non-small-cell lung cancer cell. *Cancer Res.* **2006**, *66*, 1767–1764.

(62) Rousseau, S.; Morrice, N.; Pegg, M.; Campbell, D. G.; Gaestel, M.; Cohen, P. Inhibition of SAPK2a/p38 prevents HnRNP A0 phosphorylation by MAPKAP-K2 and its interaction with cytokine MRNAs. *EMBO J.* **2002**, *21*, 6505–514.

(63) Gao, Y.; Davies, S. P.; Augustin, M.; Woodward, A.; Patel, V. A.; Kovelman, R.; Harvey, K. J. A broad activity screen in support of a chemogenomic map for kinase signaling research and drug discovery. *Biochem. J.* **2013**, *451*, 313–328.

(64) Overman, M. J.; Maru, D. M.; Charnsangavej, C.; Loyer, E. M.; Wang, H.; Pathak, P.; Eng, C.; Hoff, P. M.; Vauthey, J. N.; Wolff, R. A.; Kopetz, S. Oxaliplatin-mediated increase in spleen size as a biomarker for the development of hepatic sinusoidal injury. *J. Clin. Oncol.* **2010**, *28*, 2549–2555.

(65) Harrison, C.; Kiladjian, J. J.; Al-Ali, H. K.; Gisslinger, H.; Waltzman, R.; Stalbovskaya, V.; McQuitty, M.; Hunter, D. S.; Levy, R.; Knoops, L.; Cervantes, F.; Vannucchi, A. M.; Barbui, T.; Barosi, G. JAK inhibition with ruxolitinib versus best available therapy for myelofibrosis. *N. Engl. J. Med.* **2012**, *366*, 787–98.

(66) Gilbert, H. S. Long term treatment of myeloproliferative disease with interferon-alpha-2b: feasibility and efficacy. *Cancer* **1998**, *83*, 1205–1213.

(67) Sacchi, S. The role of alpha-interferon in essential thrombocythaemia, polycythaemia vera and myelofibrosis with myeloid metaplasia (MMM): a concise update. *Leuk. Lymphoma* **1995**, *19*, 13–20.

(68) Kuang, S.-M.; Edwards, D. A.; Fanwick, P. E.; Walton, R. A. Complexes derived from the reactions of diphenylphosphinoacetic acid. Part 3. Dimetal complexes from  $[\text{Mo}_2\text{Cl}_8]^{4-}$  and  $[\text{Re}_2\text{Cl}_8]^{2-}$ . *Inorg. Chim. Acta* **2003**, *342*, 267–271.

(69) Uson, R.; Laguna, A.; Laguna, M.; Briggs, D. A.; Murray, H. H.; Fackler, J. P. (Tetrahydrothiophene)gold(I) or gold(III) complexes. *Inorg. Synth.* **1989**, *26*, 85–91.

(70) Anastasiadis, T.; Deacon, S. W.; Devarajanm, K.; Ma, H.; Peterson, J. R. Comprehensive assay of kinase catalytic activity reveals features of kinase inhibitor selectivity. *Nat. Biotechnol.* **2011**, *29*, 1039–1046.